SEASONAL CYCLES OF PRECIPITATION AND PRECIPITABLE WATER AND THEIR USE IN MONSOON ONSET AND RETREAT

by

Er Lu

A Dissertation Submitted to the Faculty of the

DEPARTMENT OF ATMOSPHERIC SCIENCES

In Partial Fulfillment of the Requirements
For the Degree of

DOCTOR OF PHILOSOPHY

In the Graduate College

THE UNIVERSITY OF ARIZONA

2005

THE UNIVERSITY OF ARIZONA ®
GRADUATE COLLEGE

As members of the Dissertation Committee, we certify that we have read the dissertation prepared by ER LU entitled SEASONAL CYCLES OF PRECIPITATION AND PRECIPITABLE WATER AND THEIR USE IN MONSOON ONSET AND RETREAT and recommend that it be accepted as fulfilling the dissertation requirement for the Degree of DOCTOR OF PHILOSOPHY

Xubin Zeng Date: Nov 7, 2005

Steven L. Mullen Date: Nov 7, 2005

Andrew Comrie Date: Nov 7, 2005

W. James Shuttleworth Date: Nov 7, 2005

Benjamin M. Herman Date: Nov 7, 2005

Final approval and acceptance of this dissertation is contingent upon the candidate's submission of the final copies of the dissertation to the Graduate College.

I hereby certify that I have read this dissertation prepared under my direction and recommend that it be accepted as fulfilling the dissertation requirement.

Date: Nov 7, 2005

Dissertation Director: Xubin Zeng

STATEMENT BY AUTHOR

This dissertation has been submitted in partial fulfillment for an advanced degree at The University of Arizona and is deposited in the University Library to be made available to borrowers under rules of the Library.

Brief quotations from this dissertation are allowable without special permission, provided that accurate acknowledgment of source is made. Requests for permission for extended quotation from or reproduction of this manuscript in whole or in part may be granted by the head of the major department or the Dean of the Graduate College when in his or her judgment the proposed use of the material is in the interests of scholarship. In all other instances, however, permission must be obtained from the author.

SIGNED: ___ER__LU_____

ACKNOWLEDGEMENTS

I would like to thank Dr. Xubin Zeng for providing me with the opportunity to do my Ph.D in this wonderful department and my favorite research area. His help and support are very appreciated. I learned a lot from the faculty of my major and minor, especially from Drs. Benjamin Herman, James Shuttleworth, Steven Mullen, and Andrew Comrie, who are in my committee, and Drs. Philip Krider, Timothy Finan, and Roger Pielke at the Colorado State University. Dr. Michael Barlage, Cyrus Jones, and Michael Leuthold helped me a lot with computer problems. Sherry Rollins and Linda Meyers-Regal are helpful to my student life. Michael Brunke and Jesse Miller corrected my abstracts for language problems. Dr. Xiaodong Zeng, Zhuo Wang, Aihui Wang, Mark Decker, and Steve Stegall are my nice friends in both study and life. All of them are thanked greatly. Their advice, support, encouragement, and friendship are very important to the completion of my study.

I want to thank my parents and brothers, and my wife and son for their love, understanding, and encouragement. Dr. John Snavely, my (and my son's) violin teacher at Peter Howell Elementary, is also thanked along with many other friends in my living community.

DEDICATION

This dissertation is dedicated to memory all the lives lost in the hurricane Katrina that attacked the southeastern United States, especially New Orleans, in September 2005.

TABLE OF CONTENTS

TABLE OF CONTENTS - *continued*

LIST OF TABLES

LIST OF FIGURES

LIST OF FIGURES - *continued*

LIST OF FIGURES - *continued*

ABSTRACT

Precipitation (P) and precipitable water (W) are important components of the hydrological cycles in the earth system, and their seasonal cycles are closely related to monsoon circulations over monsoon regions. Through theoretical analyses and extensive analysis of data from in-situ measurements, satellite remote sensing, and regional reanalysis, significant progress has been made (via four peer-reviewed publications) in four areas related to P, W, and monsoon onset and retreat. First, based on the normalized W index, a novel unified method is proposed to determine global monsoon onset and retreat dates. The results are consistent with those obtained from different local criteria. Second, theoretical and data analyses demonstrate that, because of the large annual range of temperature, W can increase from winter to summer anywhere except in the tropics, including both monsoon and nonmonsoon regions. Third, while the seasonal variation of P is, in general, caused by complex processes (e.g., atmospheric circulations), thermodynamic derivations and data analysis demonstrate that the variation of P from winter to summer can be easily understood from the comparative strengths of the change of water vapor and the change of temperature. In monsoon regions, the change of water vapor from winter to summer is much greater than the change of temperature, so P has an in-phase relation with W. While in some of the nonmonsoon regions, where winter is the rainy season, the change of temperature is much greater than the change of water vapor,

leading to an out-of-phase relation between P and W, and, relative to summer, the coldness of the winter air is much more significant than its dryness. Finally, the satisfactory performance of the globally unified monsoon index can be understood by comparing the seasonal cycles of P and W. The significant positive correlations between P and W at seasonal and synoptic scales imply that W has the ability to indicate both the means and the interannual variations of the monsoon onset and retreat. Since large increase of W from winter to summer can occur in both monsoon and nonmonsoon regions, the global monsoon regions cannot be obtained from the seasonal change of W.

1 INTRODUCTION

Two purposes motivate this dissertation research. The first is to propose a globally unified monsoon index. Monsoons exist in North America and all other continents except Antarctica. The summer monsoon process varies greatly from year to year, which may cause severe floods and droughts. In order to mitigate the disasters and study the monsoon mechanisms, the onset and retreat dates of the monsoon are required. In the past, different definitions, criteria, and parameters have been used to determine the monsoon onset and retreat in different monsoon regions (Das 1987; Tao and Chen 1987; Hendon and Liebmann 1990; Douglas et al. 1993; Murakami and Matsumoto 1994; Li and Qu 1999; Wu and Wang 2000) and even in different parts of the same monsoon region (Higgins et al. 1999). In order to facilitate monsoon weather prediction and monsoon climate research, a globally unified index is required.

The second motivating purpose is to study the variations of precipitation and precipitable water, the dominant factors and the mechanisms involved in their variations, and their interrelationships. Water vapor plays a crucial role in the climate system as both a greenhouse gas and a hydrological component. Precipitable water, the vertical integration of water vapor, is a two-dimensional quantity just as precipitation is. Moreover, since the development of the satellite remote sensing, precipitation and

precipitable water are now both observable hydrological quantities (e.g., O'Sullivan et al. 2000). They can be assimilated into and output from atmospheric models (e.g., Mesinger et al. 2005), and both have become conventional meteorological quantities. In the atmospheric water balance equation, precipitation (mm/day) corresponds to the time change rate of precipitable water (mm), rather than the precipitable water itself. The relation between these two quantities is of a great concern to the hydroclimate community but is poorly understood. Clarification of the relation between precipitation and precipitable water in monsoon regions is the basis for understanding whether precipitable water can reasonably be adopted to determine the monsoon onset and retreat, as well as in defining global monsoon regions.

2 PRESENT STUDY

2.1 Summary

The results of the dissertation research are presented in the four articles given as appendixes. The following is a brief introduction to the unique methods designed and the new findings obtained, which represent my personal contributions in the research.

Precipitable water (W) has been used to determine the monsoon onset and retreat in India (Cadet 1986) and southern Arizona (Randel et al. 1996). In Appendix A, the annual cycle of W is used to represent the annual monsoon process, including the summer and winter monsoons and the transitions between them. The monsoon onset and retreat are regarded as phase-locked phenomena, with each corresponding to a relatively fixed stage in the annual cycle. It was initially hoped that using W, the global monsoon regions could also be determined, in addition to the monsoon onset and retreat dates. However, although global monsoon onset and retreat dates based on using this single parameter and an objective criterion are consistent with those obtained from different local criteria, the monsoon regions cannot be fully distinguished globally as hoped.

The conventional parameter used to determine the monsoon regions and monsoon onset and retreat is precipitation (P), and the difference of the tempo-spatial behaviors of the P and W is greatly concerned by the hydroclimate community. In order to confirm the reasonableness of using the W to determine the monsoon onset and retreat, and to understand why it cannot exactly identify the global monsoon regions, a comparison between the P and W was made. In Appendix B, three different seasonal patterns of P are understood from the water vapor and temperature fields. By defining the change of water vapor and change of temperature from winter to summer, the comparative significance of the changes in water vapor and temperature and their contributions to the seasonal change of P are evaluated. It is found that in areas with a winter rainy season, the change of temperature is more significant than the change of water vapor. Therefore, although water vapor is smaller than in summer, the temperature is much lower, leading to large winter precipitation.

The relation between the changes of W and surface temperature is studied in Appendix C. The W, expressed by the vertical integration of vapor pressure, can be estimated from surface temperature and relative humidity. The general relationship linking the change of W to changes in surface temperature and relative humidity is analytically established. It is shown that when there is a small increase in surface temperature, caused by synoptic processes or seasonal changes in the tropics, the influence on W can be offset by the decrease in surface relative humidity. W can increase or decrease as a result of strong convergence or divergence of the water vapor, dominated by dynamical effects in the atmosphere. Consequently, the correlation between changes

in W and surface temperature is very weak. However, when the surface temperature increases are large, as in the seasonal changes from winter to summer at mid-high latitudes, its contribution to the change in W is hard offset through normal fluctuations in the surface relative humidity. Consequently, W always increases from winter to summer, and the seasonal changes in W and surface temperature are well correlated. It is therefore suggested that the seasonal variation in W at mid-high latitudes might generally be prescribed from surface temperature, rather than merely over some ocean regions as suggested in previous research (Stephens 1990). In this paper, the change in W is also interpreted from dynamic and thermodynamic roles based on the atmospheric water balance equation.

In Appendix D, the different seasonal behaviors of P and W are used to clarify issues relating to the globally unified monsoon index. Since P and W are well and positively correlated at both the seasonal and synoptic scales over monsoon regions, it is reasonable to use W to determine the monsoon onset and retreat. However, unlike P, W has the same seasonal pattern in both monsoon and nonmonsoon regions, hence it cannot be used to defining monsoon regions globally.

2.2 Ongoing Research

This Ph.D. dissertation primarily comprises the four papers summarized above. However, as a continuation of these efforts, I am currently studying the dynamic conditions of the major precipitation regimes over the United States and Mexico and plan to prepare one additional paper, and here present some preliminary results.

2.2.1 Introduction

Lu and Zeng (2005; Appendix B) presented understanding of different precipitation seasonality regimes in terms of local atmospheric conditions (i.e., water vapor and temperature fields). Dynamic effects (e.g., circulations) are important to the formations of the precipitation seasonality regimes. In this ongoing study, favorable conditions for rainy season precipitation are being examined by contrasting rainy and dry seasons as well as the wettest and driest rainy seasons in the 25 year (1979-2003) North American Regional Reanalysis (Mesinger 2005).

2.2.2 Contrast between Rainy and Dry Seasons

Table 2.2.1 presents the 25-year (1979-2003) average monthly mean hydrological quantities for February and August over the western coast of the U.S. (WC), South Mexico (SM), and the southeastern U.S. (SE). In WC, summer evaporation is large but it

is mainly balanced by the water vapor divergence, hence precipitation is small. The large winter precipitation is mainly contributed by water vapor convergence, because evaporation is small. The situation is the same in the winter of SM but in summer of SM, precipitation is supplied by both water vapor convergence and evaporation. In summer of SE, evaporation is very strong.

Table 2.2.1: The 25-year averaged monthly mean precipitation (P), evaporation (E), and water vapor convergence (C=P-E) in February and August at WC, SM, and SE. Unit is mm/day.

Component	WC (123W/46N)		SM (105W/21N)		SE (90W/33N)	
	Feb	Aug	Feb	Aug	Feb	Aug
P	6.34	0.77	0.22	7.57	4.33	2.53
E	0.96	3.51	1.82	3.56	1.96	4.18
C	5.38	-2.74	-1.60	4.01	2.37	-1.65

Figure 2.2.1a shows the 25-year average monthly mean wind and geopotential height at 800hPa in February. The difference field between February and August is shown in Fig. 2.2.1b. The low-pressure system to the northwest of WC is very strong in winter, and the southwesterly from the ocean contributes to the rainy winter precipitation in WC.

Figure 2.2.2 presents the 25-year average monthly mean ascending motion profiles in February and August, and the correlation between the monthly mean ascending motion at a height and the monthly mean precipitation in February or August for the 25 years. In WC, ascending motion in February, the rainy season, is very strong and reaches 0.2Pa/s in magnitude at 800hPa (Fig. 2.2.2a), and the ascending motion in 800-400hPa is significantly correlated with precipitation (Fig. 2.2.2d). In SM, the ascending motion in August, the rainy season, only occurs in upper layer (above 600hPa), and is not as so strong (less than 0.1Pa/s in magnitude; Fig. 2.2.2b), but is also significantly correlated with the precipitation (Fig. 2.2.2e). The ascending motion in the SE is rather weak in both February and August (Fig. 2.2.2c). However, this weak ascending motion above 800hPa still has significant correlation with precipitation (Fig. 2.2.2f). The correlation with precipitation in these rainy months can be up to 0.8 (Figs. 2.2.2e and 2.2.2f) or 0.9 (Fig. 2.2.2d), indicating that ascending motion is important for the formation of precipitation.

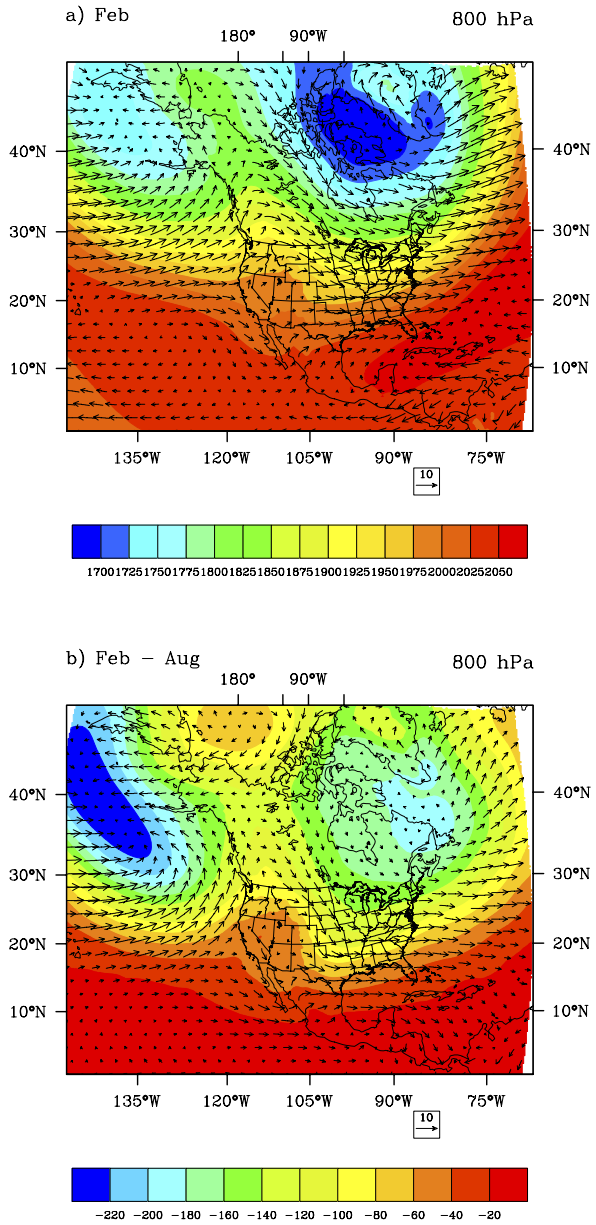

Figure 2.2.1: The 25-year averaged monthly mean wind (unit: m/s) vector and geopotential height (unit: gpm) at 800hPa. (a) In February, and (b) The difference between February and August.

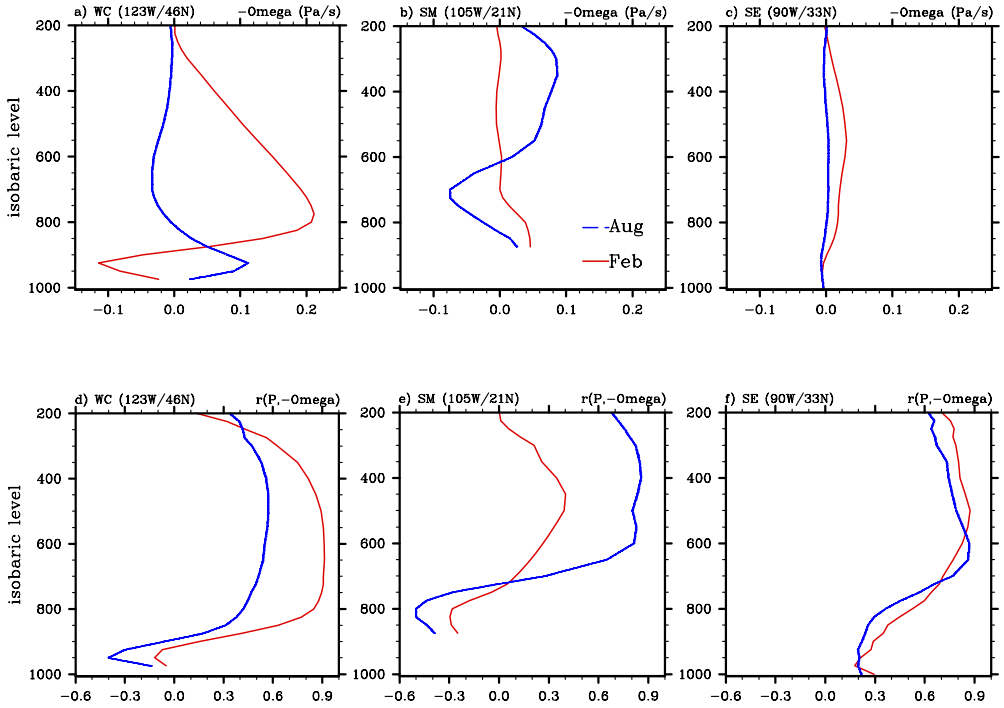

Figure 2.2.2: Profiles of (a-c) the 25-year averaged monthly mean vertical velocity (unit: Pa/s; positive value refers to upward motion); and (d-f) correlation between the 25-year time series of the monthly mean vertical velocity and precipitation in February (red) and August (blue) at WC, SM, and SE.

2.2.3 Contrast between the Wettest and Driest Rainy Seasons

Figures 2.2.3a-d show profiles of the change of water vapor and change of temperature, defined as $C_{vap} \equiv e^{wettest} / e^{driest}$ and $C_{tem} \equiv e_s(T^{wettest}) / e_s(T^{driest})$, respectively (for more details, see Appendix B), for the atmosphere between the driest rainy season and the wettest rainy season for the three regimes. In all 4 cases, temperature changes little ($C_{tem} \approx 1$), but water vapor changes a good deal ($C_{vap} > 1$), implying that the difference between the wettest and driest rainy seasons is mainly related to changes in the atmospheric water vapor. In addition, the vapor change for the two rainy summer cases (August at SM and SE; Figs. 2.2.3b and 2.2.3d) is smaller than those for the two rainy winter cases (February at WC and SE; Figs. 2.2.3a and 2.2.3c). Table 2.2.1 shows that, in February at WC and SE, water vapor convergence makes most contribution to precipitation, and accounts for 85% at WC and 55% at SE. This implies that atmospheric circulation, and related water vapor transfer, plays a significant role in rainy winter precipitation. The profiles of the change of saturation extent ($C_{sat} = C_{vap} / C_{tem}$) given in Figures 2.2.3e-h show that the increases of the saturation extent from the driest August to the wettest at SM and SE are not large (Figs. 2.2.3f and 2.2.3h). In contrast, the difference of the saturation extent between the wettest and driest February at WC and SE is very large (Figs. 2.2.3e and 2.2.3g).

Figure 2.2.4 presents the composite difference between the 6 wettest and driest Februarys at WC. There is a deep low-pressure system in the ocean just northwest of WC, and the cyclonic wind in the southeastern side of the system sweeps the WC (Fig.

2.2.4a). This low-pressure system and cyclonic circulation in the difference field between the wettest and driest rainy seasons are similar to that in the difference field of the February and August (Fig. 2.2.1). Huge amounts of water vapor are transferred to the WC (Fig. 2.2.4b), and this convergence (Fig. 2.2.4c) is adjacent to the precipitation (Fig. 2.2.4d), with respect to both geographic extent and magnitude.

In February at SE (Fig. 2.2.5), the low-pressure system is located over the southwestern U.S. and the northern Mexico, and the cyclonic wind to the east of the system passes through the SE (Fig. 2.2.5a). The water vapor flux over the Golf of Mexico is very strong (Fig. 2.2.5b), causing maximal vapor convergence in the SE (Fig. 2.2.5c), and this makes a major contribution to precipitation (Fig. 2.2.5d).

In summer of SM, although evaporation is an important water vapor source (Table 2.2.1), dominating pressure systems can also be found in the difference fields (figures not shown).

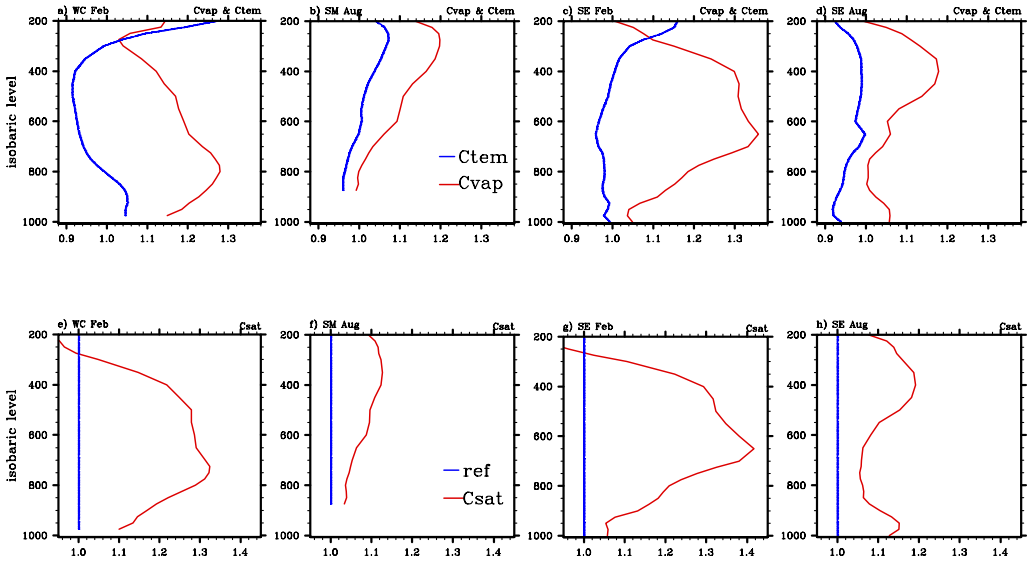

Figure 2.2.3: Profiles of (a-d) the change of water vapor (C_{vap}, red) and the change of temperature (C_{tem}, blue) between the averaged monthly means of the 6, of the 25-years, driest and wettest rainy Februarys at WC, Augusts at SM, Februarys at SE, and Augusts at SE, respectively; and (e-h) the change of saturation extent (C_{sat}, red) and a reference line of 1.0 (blue) at WC, SM, and SE.

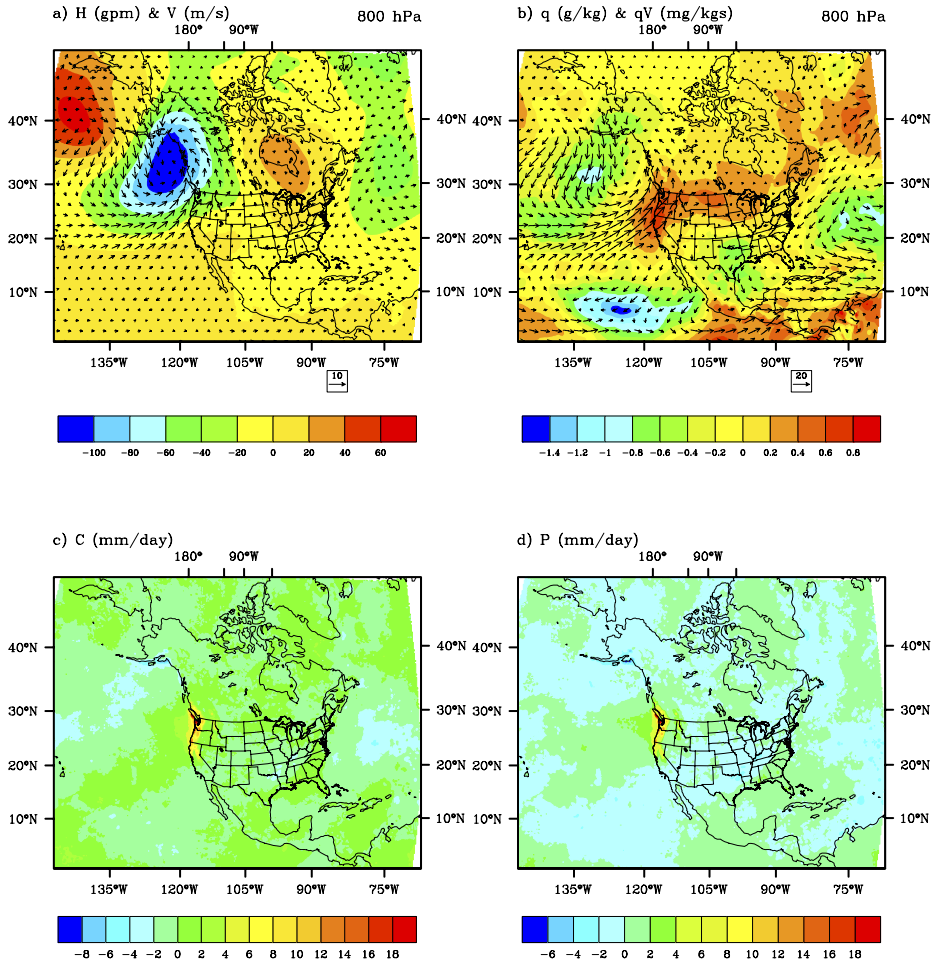

Figure 2.2.4: Differences of the composites of the 6 wettest and driest Februarys at WC for (a) geopotential height (gpm) and wind (m/s) vector at 800hPa; (b) specific humidity (g/kg; shaded) and water vapor flux (gm/kgs; vector) at 800hPa; (c) column integrated water vapor flux convergence (mm/day); and (d) monthly precipitation (mm/day).

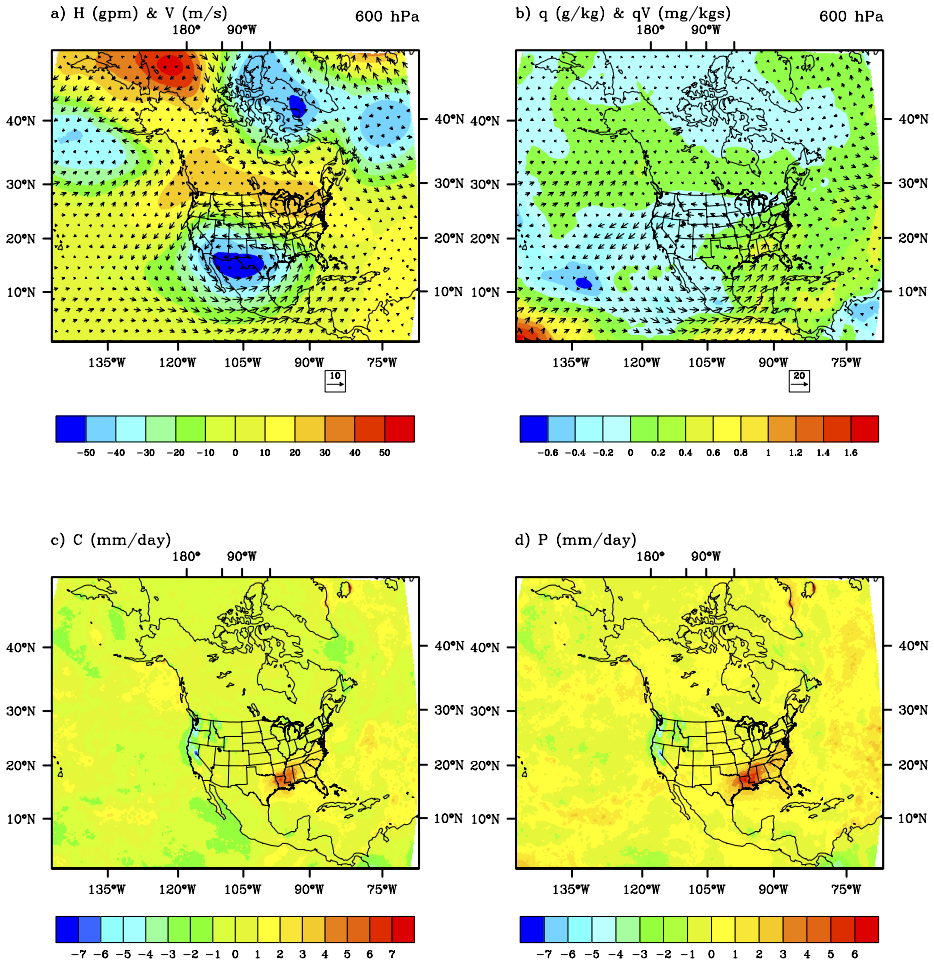

Figure 2.2.5: Same as in Fig. 2.2.4 except for SE and 600hPa in (a) and (b).

2.2.4 Possible Teleconnetions

When analyzing these data, we noticed that teleconnections might also exist between the precipitations in different seasons and different regions. For example, the February precipitation at WC has a significant negative correlation with the August precipitation at SE (r=-0.41), while the February precipitation at SE has a significant positive correlation with the August precipitation at SM (r=0.42). These lagged relationships may have some prediction value at the seasonal timescale, but additional data analyses are still required to investigate these relationships, and the underlying mechanisms responsible for these phenomena need to be better understood.

3 REFERENCES

Cadet, D. L., 1986: Fluctuations of precipitable water over the Indian Ocean during the 1979 summer monsoon. *Tellus.,* 38A, 170–177.

Das, P. K., 1987: Short- and long-range monsoon prediction in India. *Monsoons,* J. S. Fein and P. L. Stephens, Eds., John Wiley & Sons, 549–778.

Douglas, M., Maddox R. A., Howard K., and Reyes S., 1993: The Mexican monsoon. *J. Climate.,* 6, 1665–1677.

Hendon, H. H., and Liebmann B., 1990: A composite study of onset of the Australian summer monsoon. *J. Atmos. Sci.,* 47, 2227–2240.

Higgins, R. W., Chen Y., and Douglas A. V., 1999: Interannual variability of the North American warm season precipitation regime. *J. Climate.,* 12, 653–680.

Li, C., and Qu X., 1999: Atmospheric circulation evolutions associated with summer monsoon onset in the south China Sea. *Chin. J. Atmos. Sci.,* 23, 311–325.

Lu, E., and X. Zeng, 2005: Understanding different precipitation seasonality regimes from water vapor and temperature fields: Case studies. *Geophys. Res. Lett.*, in press.

Mesinger, F., et al. (2005), North American Regional Reanalysis, *Bull. Am. Meteorol. Soc.*, submitted.

Murakami, T., and Matsumoto J., 1994: Summer monsoon over the Asian continent and western North Pacific. *J. Meteor. Soc. Japan.,* 72, 719–745.

O'Sullivan, D. B., B. M. Herman, D. Feng, D. E. Flittner, and D. M. Ward (2000), Retrieval of water vapor profiles from GPS/MET radio occultations, *Bull. Am. Meteorol. Soc.*, *81*, 1031–1040.

Randel, D. L., T. J. Greenwald, T. H. V. Haar, et al., 1996: A new global water vapor dataset, *Bull. Am. Meteorol. Soc.*, *77*, 1233–1254.

Stephens, G. L., 1990: On the relationship between water vapor over the oceans and sea surface temperature. *J. Climate.*, *3*, 634–645.

Tao, S., and Chen L., 1987: A review of recent research on the East Asian summer monsoon in China. *Monsoon Meteorology,* C.-P. Chang and T. N. Krishnamurti, Eds., Oxford University Press, 60–92.

Wu, R., and Wang B., 2000: Interannual variability of summer onset over the western North Pacific and the underlying processes. *J. Climate.,* 13, 2483–2501.

APPENDIX A

GLOBALLY UNIFIED MONSOON ONSET AND RETREAT INDEXES

XUBIN ZENG and ER LU

Department of Atmospheric Sciences
The University of Arizona
Tucson, Arizona

Published in

Journal of Climate

June 2004, Volume 17, pp 2241-2248

A.1 Abstract

Different criteria have been used in the past to define the monsoon onset and retreat over different monsoon regions and even over different parts of the same monsoon region. Here an objective criterion is proposed to define, for the first time, globally unified summer monsoon onset (or retreat) dates using a single meteorological variable (i.e., the global daily 1° × 1° normalized precipitable water data) with the threshold value being the Golden Ratio (0.618). Results are found to be consistent with those determined using long-term rainfall data over most monsoon regions. The precipitable water data have also been used to refine the definition of monsoon regions on a grid-cell-by-cell basis. The objective definitions of these basic monsoon characteristics would provide one of the necessary foundations for global monsoon research. They, along with the onset/retreat data over a 10-yr period (1988–97), would also facilitate the diagnostics and validation of global monsoon simulations.

A.2 Introduction

Monsoon is one of the key elements of the global climate system and strongly affects agricultural and other human activities in monsoon regions (e.g., Webster et al. 1998). The basic monsoon characteristics, such as onset, retreat, and geographical extent, have been studied for decades (e.g., Ramage 1971). The most fundamental driving mechanisms of a monsoon system include the differential heating of the land and ocean; the moist processes that determine the strength, vigor, and location of the major monsoon precipitation; and the rotation of the earth (Webster 1987). The seasonal reversal of wind direction over monsoon regions (e.g., India) has been noted for thousands of years (Warren 1987), while the attempt to understand monsoon meteorology based on physical principles began over 300 years ago (Kutzbach 1987). The onset of the summer monsoon is generally concurrent with a reversal or major change in the wind field, an abrupt rise in precipitation and water vapor, and a drastic change in other variables (e.g., kinetic energy). Partly for this reason, different criteria have been used to define the monsoon onset and retreat over different monsoon regions (Das 1987; Tao and Chen 1987; Hendon and Liebmann 1990; Douglas et al. 1993; Murakami and Matsumoto 1994; Li and Qu 1999; Wu and Wang 2000) and even over different parts of the same monsoon region (Higgins et al. 1999).

The purpose of this paper is to propose a simple, yet objective criterion to define globally unified summer monsoon onset or retreat dates using daily precipitable water data. The same data will also be used to refine the definition of monsoon regions on a grid-cell-by-cell basis. These objective definitions of monsoon onset, retreat, and extent would provide one of the necessary building blocks for global monsoon study. They, along with the onset/retreat data for 10 yr (1988–97), would also facilitate the diagnostics and validation of global monsoon simulations.

A.3 Data and Proposed Criterion

Three different datasets have been widely used to study monsoon onset and retreat in the past: surface meteorological station data (e.g., precipitation, dewpoint temperature), radiosonde data (e.g., wind field), and satellite outgoing longwave radiation (OLR) data. However, each of these datasets has serious limitations; for instance, the relationship between OLR data and precipitation over land is not as good as that over ocean; and the relationship becomes much worse at daily time scales (e.g., Xie and Arkin 1998; Wu and Wang 2000). Precipitable water (W) data were used over the Indian Ocean during the 1979 summer monsoon (Cadet 1986). More recently, the climatological pentad (5 day) mean rainfall data, which were derived by merging the satellite estimates, surface gauge measurements, and numerical model outputs (Xie and Arkin 1997), were used to study the rainy season of the Asian–Pacific summer monsoon (Wang and LinHo 2002).

Here we intend to use the global daily W data on 1° × 1° grids from January 1988 to December 1997 (Randel et al. 1996). These data combine water vapor retrievals from satellite infrared and microwave sensors with radiosonde data, and hence are well-suited for the study of the short-term and intraseasonal variability of monsoon (including its onset and retreat). As mentioned earlier, the abrupt rise (or decrease) of water vapor is one of the features associated with the monsoon onset (or retreat). Furthermore, the quantitative relationship between precipitation, cloud-top temperature, and W between 40°N and 40°S has been established (Zeng 1999).

First a normalized precipitable water index (NWI) is defined:

$$NWI = \frac{W - W_{\min}}{W_{\max} - W_{\min}} \tag{A1}$$

where W is the daily precipitable water at each 1° × 1° grid, and W_{max} and W_{min} are the 10-yr averages of the annual maximum and minimum daily W at each grid, respectively.

Table A.1: The median, mean, 25th percentile ($q_{0.25}$), and 75th percentile ($q_{0.75}$) of the annual maximum daily W (W_{max}) and minimum values (W_{min}) during the 10-yr period (1988–97) over seven 1° × 1° grid cells over Bombay, India (centered at 19.5°N, 72.5°E), the southeast coast of China (23.5°N, 114.5°E), the western North Pacific (13.5°N, 112.5°E), southern Arizona (31.5°N, 111.5°W), North Africa (15.5°N, 10.5°W), Darwin, Australia (12.5°S, 129.5°E), and South America (22.5°S, 55.5°W), respectively. These seven cells are also marked in Figs. A.2 and A.3.

	PW_{max} (mm)				PW_{min} (mm)			
	Median	Mean	$q_{0.25}$	$q_{0.75}$	Median	Mean	$q_{0.25}$	$q_{0.75}$
India	76	77	74	80	8	9	8	10
China	70	71	70	71	12	11	10	13
North Pacific	73	73	67	80	21	21	20	22
Arizona	45	45	44	45	3	4	3	4
North Africa	59	61	56	66	11	11	10	12
Australia	73	72	67	77	10	9	8	10
South America	52	53	51	55	10	9	8	10

Table A.1 shows that, at the selected seven grid cells, the 10-yr mean and median W_{max} values are within 2 mm, and the mean and median W_{min} values are within 1 mm. The interquartile range (i.e., the difference between the 75th and 25th percentiles), which is a more robust and resistant measure of spread than standard deviations, varies from 1 to 13 mm for W_{max}, and is within 3 mm for W_{min} over different cells. In contrast, the difference of W_{max} (or W_{min}) over different regions can be much larger (e.g., 31 mm for W_{max} between Bombay, India, and southern Arizona; and 18 mm for W_{min} between the western North Pacific and southern Arizona).

Using NWI, we propose the following objective criterion to define the globally unified summer monsoon onset (or retreat) date:

The summer monsoon onset (or retreat) date for grid cell G is defined as the first day (d) when NWI is greater (or less) than the Golden Ratio (0.618) for three consecutive days in seven of the nine cells centered at cell G in day d or (d ± 1).[1]

[1] If one or more of the nine grids are undefined, for example, at the edge of monsoon regions, the required number of seven is correspondingly reduced. For instance, if only seven grid cells are defined, the required number is five.

This criterion is objective in the sense that all parameters are fixed and hence no subjective error is involved. However, the selection of these parameters is somewhat subjective, just as in previous studies (e.g., Murakami and Matsumoto 1994; Higgins et al. 1999; Wu and Wang 2000). For instance, the National Weather Service in Arizona defines the monsoon onset date as the first day when the near-surface air dewpoint temperature is greater than 55°F (or 13°C) for three consecutive days. Higgins et al. (1999) took the first day after 1 May (when the daily precipitation is greater than 0.5 mm day^{-1} for three consecutive days) as the onset date in Arizona and New Mexico. Similarly, we consider "three consecutive days" in our criterion. Because the monsoon onset represents a large-scale change of weather patterns, data over multiple stations are usually used to define monsoon onset over a given region [e.g., by the Indian Meteorological Department; Mooley and Shukla (1987)]. Similarly, we consider "nine cells" in our criterion to help remove the spurious early onset over one or more cells due to the intraseasonal variability (e.g., in precipitation and water vapor) during the premonsoon period (Flatau et al. 2001). This would also largely remove the spurious early onset over isolated cells partly due to our use of the original (i.e., unfiltered) daily W data. Note that, even though most previous studies used a smoothed annual cycle (e.g., of OLR) to define monsoon onset (Murakami and Matsumoto 1994; Wu and Wang 2000), their use of a single grid cell (without considering adjacent cells) might be an important reason for the spatial discontinuity in their defined monsoon onset dates (e.g., Fig. 6 of Wang and LinHo 2002).

Compared with the onset and retreat dates based on local precipitation data that are available over various monsoon regions in different years, we found that the monsoon onset and retreat are always corresponding to a roughly fixed stage of the annual cycle of W, even though both W_{max} and W_{min} are quite different over different regions (see Table A.1). Specifically, a threshold value of 0.6–0.63 for NWI was found to work adequately. For instance, Fig. A.1 shows that the two cells in Bombay, India, and southern Arizona have significantly different W_{max} values and hence quite different threshold W values that mark the monsoon onset. However, these threshold W values both correspond to a similar value of NWI. Because the Golden Ratio $[((5)^{1/2} - 1)/ 2 = 0.618]$ (e.g., Livio 2002) falls within the range of 0.6 to 0.63 and is, after all, present in many natural growth patterns (probably including the evolution of monsoons), it is chosen as the threshold value in our criterion. Its use here, however, does not imply that all the decimal points associated with this irrational number are needed.

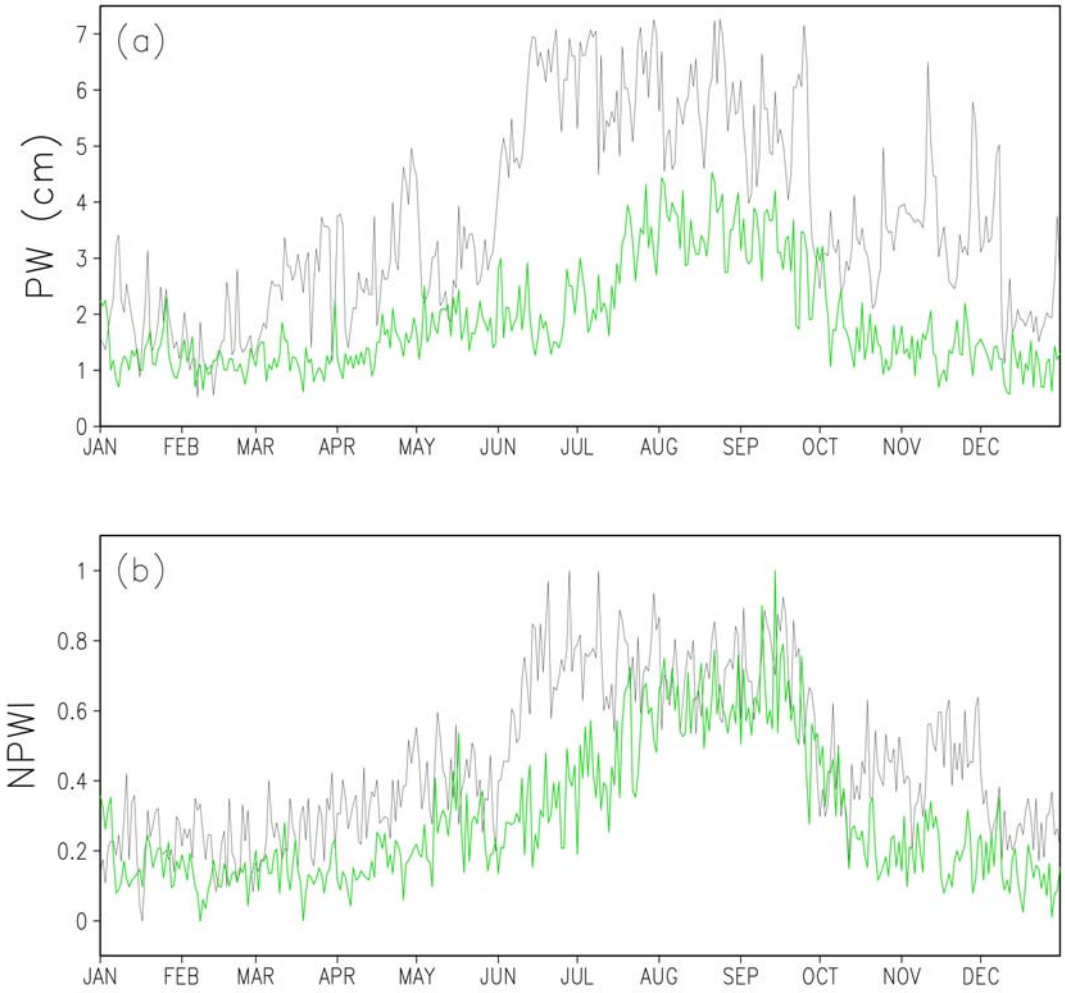

Figure A.1: (a) The 10-yr-averaged daily W over Bombay, India (centered at 19.5°N, 72.5°E, denoted by black lines), and over southern Arizona (31.5°N, 111.5°W, denoted by green lines). (b) The corresponding annual cycle of the normalized W index as defined in Eq. (A1).

A.4 Results

A.4.1 Geographic extent of monsoon

As mentioned earlier, over monsoon regions where W is relatively high during the wet summer and relatively low during the dry winter, the use of NWI leads to a single threshold value (i.e., the Golden Ratio) in our criterion. Over nonmonsoonal regions with relatively small ($W_{max} - W_{min}$), however, the use of NWI may amplify small variations in W. Also, some nonmonsoonal regions (e.g., Illinois) have a relatively large ($W_{max} - W_{min}$) and an abrupt rise of W in early summer. In both of these nonmonsoonal regions, our criterion would give spurious monsoon onset and retreat dates. Therefore, W itself is not sufficient to distinguish between monsoonal and nonmonsoonal regions, and our criterion should be applied to monsoon regions only.

A consensus on the global geographical extent of monsoon has not been reached yet. Using a rather strict definition of a monsoon based on both wind reversal and seasonal precipitation criteria, Ramage (1971) identified only African, Asian, and Australian regions as monsoon regions (35°N–25°S, 30°W–170°E). Higher latitudes over east Asia have also been included in recent studies (e.g., Wang and LinHo 2002). Later, justification was given for considering North America as a monsoon region based on the seasonal precipitation criterion and the seasonal surface wind reversal over some areas (Douglas et al. 1993; Higgins et al. 1999). Zhou and Lau (1998) also suggested that South America qualifies as a monsoon region based on the seasonal precipitation criterion and

the fact that the wind reversal becomes apparent after the strong annual mean wind is removed. These studies, however, are not sufficient for our analysis of the 1° × 1° W data, because we need to define monsoon regions on a grid-cell-by-cell basis. For instance, the exact geographic extent of monsoon over South America was not given by Zhou and Lau (1998). In contrast, the monsoon regions as defined by Ramage (1971) contain many nonmonsoonal cells over the interior of the Sahara Desert, over the Tibetan Plateau, and near the equator.

To refine the definition of monsoon regions on a grid- cell-by-cell basis, we first compute the 10-yr-averaged monthly W over each cell. Then we obtain the maximum monthly W during the three summer months [e.g., June–August in the Northern Hemisphere (NH), denoted as W_w], and the maximum monthly W during the three winter months (e.g., December–February for the NH, denoted as W_c). The refined monsoon regions are simply defined as grid cells that are within the monsoon regions given in the above studies and have a difference between W_w and W_c greater than 12 mm. Initially we have also tried to use the annual maximum and minimum monthly W values. They would give similar results over known monsoon regions with relatively high W during the wet summer and relatively low W during the dry winter. However, they would also include some nonmonsoonal regions, particularly over the equatorial regions (figure not shown). For instance, for a grid cell centered at (2.5°S, 10.5°W) over the equatorial Atlantic, the difference between the annual maximum (50 mm in April) and minimum (30 mm in July) monthly W values is as large as that over monsoon regions (e.g., Fig. A.1). In contrast,

the difference between W_w (45 mm in February) and W_c (34 mm in June) is less than 12 mm, and hence this grid cell is defined as nonmonsoonal.

The monsoon regions defined in this way are indicated as unshaded areas in Figs. A.2 and A.3. Grid cells over the Sahara Desert and the Tibetan Plateau are correctly masked. Similarly, cells over the Sierra Madre Occidental in Mexico are masked, even though the number of shaded cells seems to be slightly larger than indicated in Higgins et al. (1999). Also shaded are nearly all cells between 8°N and 8°S, including some regions with well- known seasonal reversal of wind direction (e.g., along the coast of Somalia). This is not surprising, because monsoon regions that are defined based on wind versus precipitation data could also be different. The geographic extent of the South American monsoon was not provided in Zhou and Lau (1998), and is shown to be relatively small compared with other known monsoon regions in Figs. A.2 and A.3. Most of the continental United States, the Gulf of Mexico, and southern Africa have ($W_w - W_c$) greater than 12 mm, but they are generally regarded as nonmonsoonal from previous studies and hence are shaded as well.

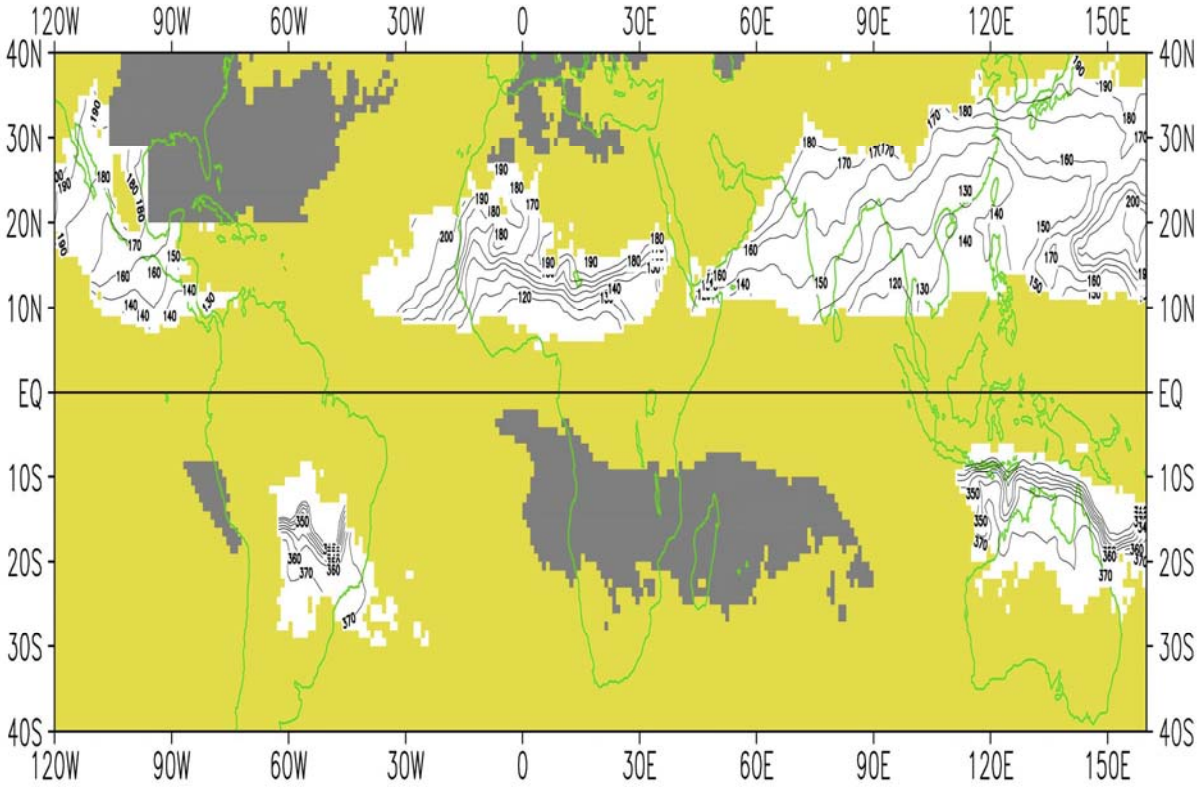

Figure A.2: The global distribution at 1° × 1° resolution of the median dates (in Julian day) of summer monsoon onset between 1988 and 1997. A number (n) greater than 365 represents the Julian day ($n - 365$) in the following year. Monsoon regions are indicated by unshaded grid cells, and the seven cells used in Tables A.1 and A.2 are also marked. Yellow (or gray) shades indicate nonmonsoonal grid cells with relatively small (or large) annual cycle of W.

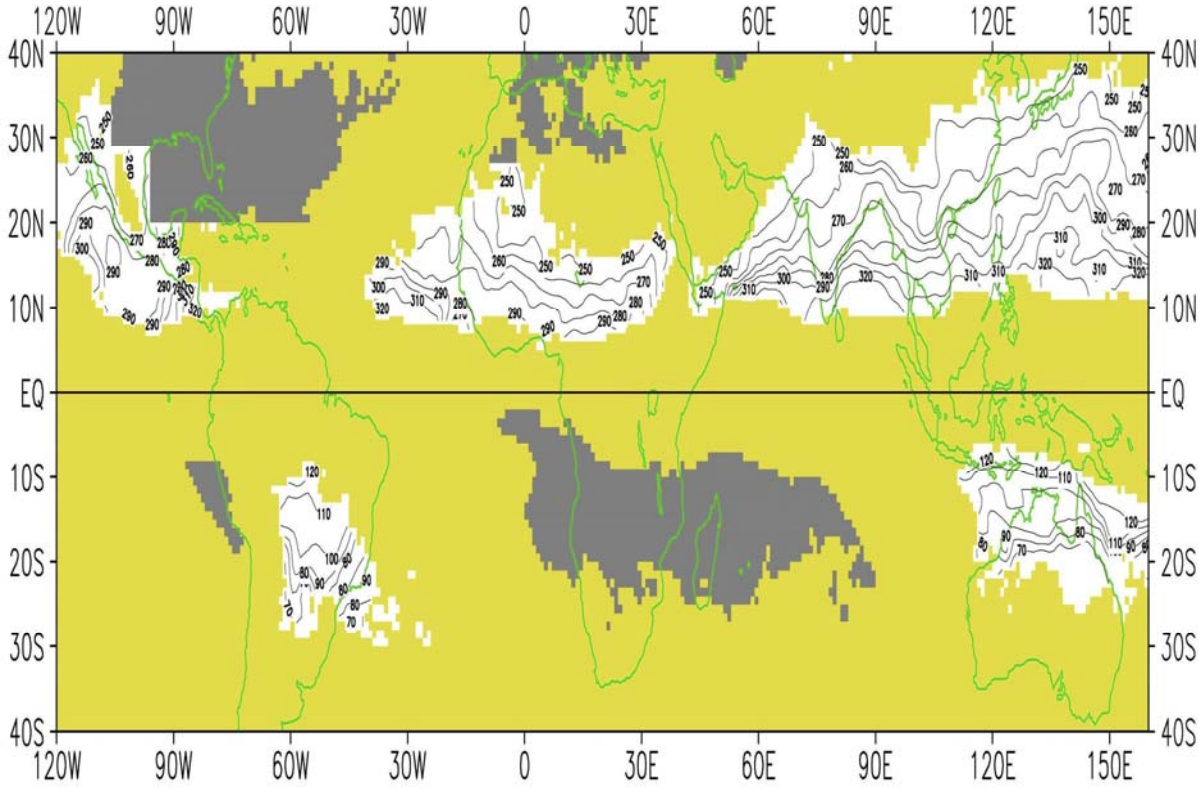

Figure A.3: Same as in Fig. A.2 except for the median dates (in Julian days) of summer monsoon retreat between 1988 and 1997.

A.4.2 Monsoon onset and retreat dates

Figures A.2 and A.3 show the global distribution of median monsoon onset and retreat dates during the 10-yr period. In the NH, the onset of the summer monsoon starts in early to mid-May [Julian Day (JD) 120–140] and reaches the edge of different monsoon regions by mid-July (around JD190). The summer monsoon commences withdrawal in early September (JD250), and retreats from most monsoon regions by late October (JD300). In the Southern Hemisphere, the corresponding onset and retreat dates differ from those in NH by about 6 months.

In general, summer monsoon onset is associated with the dry to wet transition (e.g., in precipitation, W, or OLR) and the wind direction reversal. Over a specific area, however, the exact onset dates based on dry to wet transition and wind reversal are not necessarily simultaneous; rather, they could be significantly different (e.g., Das 1987; Webster 1987; Murakami and Matsumoto 1994; Wang and LinHo 2002). The W is primarily related to the dry to wet transition, and our results should be compared primarily with those based on precipitation or OLR data.

In Asia, the summer monsoon occurs first in a band across the Indochina peninsula in early May (JD120– 130), consistent with results based on the OLR data (Wu and Wang 2000). It then progresses northwestward into the Indian subcontinent (through the Bay of Bengal), northward in East Asia, and eastward in the western North Pacific (including the South China Sea and the Philippine Sea). The summer monsoon arrives in southern India in late May (JD140–150), rapidly spreads to most of the country within 30

days, and reaches the foothills of the Tibetan Plateau in early July (around JD180). It commences withdrawal in early September (around JD250) and retreats from most of the continent (except south peninsular India) by mid-October (JD290–300). The onset and retreat patterns in India as shown in Figs. A.2 and A.3 are nearly the same as those prepared by the Indian Meteorological Department based on average pentad rainfall data (Mooley and Shukla 1987). Table A.2 shows that the average onset (or retreat) dates over Bombay, India, are within two days of those given in Mooley and Shukla (1987).

In east Asia, Fig. A.2 shows that the summer monsoon advances to southern China in mid-May (JD130–140; also Table A.2), and reaches the Yangtze River valley in mid-June (JD160–170) when the mei-yu (i.e., so-called plum rain) in the valley and the baiu in Japan begin. Then the monsoon progresses slowly northward for the next three weeks to cover part of northern China, South Korea, and Japan, consistent with the stagnant mei-yu front. Figure A.3 shows that the monsoon starts withdrawal in early September (around JD250), and rapidly retreats from the mainland of China in a month. These results over east Asia are nearly the same as those determined using long-term rainfall records (Tao and Chen 1987).

Table A.2: The median, mean, 25th percentile ($q_{0.25}$), and 75th percentile ($q_{0.75}$) of the summer monsoon onset and retreat dates during the 10-yr period (1988–97) over the same seven grid cells as in Table A.1. The values in parentheses are the corresponding onset/retreat dates from Mooley and Shukla (1987) (over India), Tao and Chen (1987) (China), Wang and LinHo (2002) (the North Pacific), Higgins et al. (1999) (Arizona), and Hendon and Liebmann (1990) (Australia).

	Onset date				Retreat date			
	Median	Mean	$q_{0.25}$	$q_{0.75}$	Median	Mean	$q_{0.25}$	$q_{0.75}$
India	159 (161)	158	155	162	271 (271)	271	257	286
China	131 (130)	132	122	139	268	267	258	276
North Pacific	139 (133)	139	132	147	312 (333)	315	296	336
Arizona	188 (187)	191	186	198	249	250	246	251
North Africa	151	156	143	171	267	271	261	285
Australia	362 (359)	341	305	362	99	96	92	104
South America	9	14	6	16	56	62	47	86

Just as in east Asia, the summer monsoon progression is stepwise in the western North Pacific. It rapidly spreads to the South China Sea and the Philippine Sea by mid- to late May (JD130–150), followed by slow eastward movement until early July (JD190). Then it advances rapidly eastward again. This stepwise progression is consistent with those using the pentad satellite precipitation data (Wang and LinHo 2002). Table A.2 shows that, at the grid cell centered at (13.5°N, 112.5°E) over the South China Sea, our onset date of JD139 is close to their pentad 37 (JD 133). The earlier onset over the northern (than over the southern) South China Sea is also consistent with Lau et al. (2000). Over the eastern Philippine Sea, however, these results based on W or precipitation are significantly different from those based on the OLR data in Murakami and Matsumoto (1994). Figure A.3 shows that the monsoon begins withdrawal from the western North Pacific by mid-October (JD280–290), and retreats from this region by mid-November (JD320). The overall patterns of monsoon retreat using the daily W data (Fig. A.3), pentad satellite precipitation data (Wang and LinHo 2002), or pentad OLR data (Murakami and Matsumoto 1994) are somewhat different. For instance, Table A.2 shows that our median retreat date around (13.5°N, 112.5°E) is JD312, while Wang and LinHo (2002) gave pentad 67 (JD333).

The North American monsoon system (NAMS) refers to the monsoon over Mexico and the southwestern United States (Douglas et al. 1993; Higgins et al. 1999). Figure A.2 shows that the summer monsoon actually starts from Central America in late May (JD140–150), reaches southern Mexico by early June (JD160), and advances to the southwestern United States by early July (JD190). It begins withdrawal by early

September (JD250), and retreats from North America in 1 month (Fig. A.3). These results are consistent with those based on long-term in situ precipitation data (Higgins et al. 1999). For instance, over southern Arizona (31.5°N, 111.5°W), our median onset date is JD188 versus JD187 in Higgins et al. Both are also consistent with JD186 as determined by the National Weather Service in Arizona using the dewpoint temperature data. Note that while different threshold values and durations were used over southwestern United States, northern Mexico, and southern Mexico, respectively, in Higgins et al., all parameters remain the same globally in our criterion.

Over North Africa, Fig. A.2 shows that the summer monsoon onset occurs in early May (JD120–130) and advances northward slowly toward the southern edge of the Sahara Desert in the interior of the continent. Only over West Africa, does the monsoon advance northward well beyond 15°N. The monsoon starts withdrawal by mid-September (JD250) and retreats from the continent in a month (Fig. A.3). Table A.2 indicates that the median onset and retreat dates at the grid cell centered at (15.5°N, 10.5°W) are JD151 and JD267, respectively.

Over Australia and Indonesia, Fig. A.2 shows that the summer monsoon sets in by early November (JD310) and reaches northern Australia by late December and early January (JD370). Its withdrawal starts by early March (JD70) and terminates by late April (JD120) (Fig. A.3). Compared with the average onset date (JD359) in Darwin (12°S, 130°E) based on local rainfall and wind data (Hendon and Liebmann 1990), our median onset date is very close (JD362), while the average date using the pentad OLR

data (Murakami and Matsumoto 1994) is much earlier (around JD328 from their Fig. A.3).

Over subtropical South America, Fig. A.2 shows that the summer monsoon occurs in early November (around JD310) and advances slowly southward until mid-December (JD350). It then spreads rapidly and reaches the coast of southern Brazil in early January (JD370). The monsoon withdrawal starts in mid-March (around JD80) and ends in late April (JD120).

A.5 Conclusions and Further Discussions

Wind, precipitation, and OLR data have been traditionally used for monsoon research. Here daily W data are introduced as a new global variable to study monsoon onset and retreat. Furthermore, a simple, yet objective criterion based on daily W is proposed to define summer monsoon onset and retreat dates over different monsoon regions in the world. Overall, the results are consistent with those using local precipitation data over most monsoon regions. Over the western North Pacific and particularly over the eastern Philippine Sea, monsoon retreat (and to certain degree onset) dates are calculated to be quite different, depending on the use of daily W data, pentad satellite precipitation data (Wang and LinHo 2002), or pentad OLR data (Murakami and Matsumoto 1994). This disagreement suggests the need for further study using in situ data (e.g., buoys). Over Australia, the daily W data and pentad OLR data (Murakami and Matsumoto 1994) also give different onset and retreat dates. Furthermore, Table A.2

shows a difference of 20 days between the median and mean onset dates over this region and an interquartile range of 57 days of the onset dates during the 10-yr period. These large differences may be related to the inherent difficulty in distinguishing premonsoon activities from monsoon onset over this region (e.g., Hendon and Liebmann 1990).

The geographic extent of monsoon regions has been defined by various researchers in the past, but it is difficult to apply their results to individual 1° × 1° grid cells. Even though W itself is not sufficient to distinguish between monsoonal versus nonmonsoonal regions, its use over grid cells within the monsoon regions identified in previous studies enables us to refine the definition of monsoon regions on a grid-cell-by-cell basis, as indicated by the unshaded regions in Figs. A.2 and A.3. In particular, our study provides the geographic extent of the South American monsoon that was not determined in previous studies (e.g., Zhou and Lau 1998). While southern Africa, most of the continental United States, and the Gulf of Mexico are generally regarded as nonmonsoonal, they still have relatively large annual cycle of W and well-defined dates for the abrupt increase of W in early summer and decrease of W in early fall. We are currently analyzing the daily precipitation and W data over North America to compare and understand the relationship between precipitation and W over Mexico and the southwestern United States versus that over other nonmonsoonal regions.

In general, the temporal variation of precipitation, water vapor, and wind fields during the summer monsoon retreat is less drastic than that during the monsoon onset. It is also difficult to distinguish the summer monsoon retreat from the winter monsoon

onset. Therefore, the summer monsoon retreat dates (particularly over low latitudes) using the W (Fig. A.3), satellite precipitation (Fig. 8 of Wang and LinHo 2002), or OLR data (Fig. 3 of Murakami and Matsumoto 1994) may not be as reliable as the onset dates, and hence should be used with caution.

It needs to be emphasized that monsoon onset and retreat dates may vary significantly from year to year at some locations. For instance, Table A.2 shows that the interquartile range of onset dates between 1988 and 1997 varies from 7 to 57 days in seven 1° × 1° grid cells selected over different monsoon regions. The interquartile range of retreat dates also varies from 5 to 40 days. Considering the observed large interannual variability in monsoon onset and retreat (e.g., Mooley and Shukla 1987) and results in Table A.2, the interannual variability in monsoon onset and retreat dates based on 10 yr worth of W data in our study should be viewed as preliminary and updated whenever longer-term data become available. Furthermore, while the unified criterion in this paper provides a necessary building block for global monsoon study, much work is still needed to provide additional insights (from the W seasonal variation) about the operation of monsoon system. As an example, work is currently under way to understand the impact of various factors (e.g., El Niño) on the interannual variability of the monsoon onset and retreat dates and the potential value of this interannual variability in predicting summer precipitation over monsoon regions.

Another potential application of our results is the evaluation of global monsoon simulations. Most climate models are deficient in simulating global monsoons (e.g.,

Sperber and Palmer 1996). While monsoon precipitation and circulations have been emphasized in model evaluations, global monsoon onset and retreat in model simulations have not received much attention. The simple and objective definitions of monsoon onset, retreat, and extent in this paper can be directly applied to the daily W output of any global model. Model results can then be evaluated using the monsoon onset and retreat data here.

A.6 Acknowledgments

This work was supported by NOAA under Grants NA06GP0569 and NA16GP1619 and NASA through its EOS IDS Program (429-81-22; 428-81-22). We thank Mike Barlage, Bob Maddox, Ben Herman, Andrew Comrie, Chongyin Li, and three anonymous reviewers for helpful comments. The precipitable water data are distributed by the Distributed Active Archive Center (DAAC) at the NASA Langley Research Center.

A.7 References

Cadet, D. L., 1986: Fluctuations of precipitable water over the Indian Ocean during the 1979 summer monsoon. *Tellus.,* 38A, 170–177.

Das, P. K., 1987: Short- and long-range monsoon prediction in India. *Monsoons,* J. S. Fein and P. L. Stephens, Eds., John Wiley & Sons, 549–778.

Douglas, M., Maddox R. A., Howard K., and Reyes S., 1993: The Mexican monsoon. *J. Climate.,* 6, 1665–1677.

Flatau, M. K., Flatau P. J., and Rudnick D., 2001: The dynamics of double monsoon onsets. *J. Climate.,* 14, 4130–4146.

Hendon, H. H., and Liebmann B., 1990: A composite study of onset of the Australian summer monsoon. *J. Atmos. Sci.,* 47, 2227–2240.

Higgins, R. W., Chen Y., and Douglas A. V., 1999: Interannual variability of the North American warm season precipitation regime. *J. Climate.,* 12, 653–680.

Kutzbach, G., 1987: Concepts of monsoon physics in historical perspective: The Indian monsoon (seventeenth to early twentieth century). *Monsoons,* J. S. Fein and P. L. Stephens, Eds., John Wiley & Sons, 159–210.

Lau, K.-M., and Coauthors, 2000: A report of the field operations and early results of the South China Sea Monsoon Experiment (SCSMEX). *Bull. Amer. Meteor. Soc.,* 81, 1261–1270.

Li, C., and Qu X., 1999: Atmospheric circulation evolutions associated with summer monsoon onset in the south China Sea. *Chin. J. Atmos. Sci.,* 23, 311–325.

Livio, M., 2002: *The Golden Ratio: The Story of Phi, the World's Most Astonishing Number*. Broadway Books, 304 pp.

Mooley, D. A., and Shukla J., 1987: Variability and forecasting of the summer monsoon rainfall over India. *Monsoon Meteorology,* C.-P. Chang and T. N. Krishnamurti, Eds., Oxford University Press, 26–59.

Murakami, T., and Matsumoto J., 1994: Summer monsoon over the Asian continent and western North Pacific. *J. Meteor. Soc. Japan.,* 72, 719–745.

Ramage, C., 1971: *Monsoon Meteorology*. Academic Press, 296 pp.

Randel, D. L., Vonder Haar T. H., Ringerud M. A., Stephens G. L., Greenwald T. J., and Combs C. L., 1996: A new global water vapor dataset. *Bull. Amer. Meteor. Soc.,* 77, 1233–1246.

Sperber, K. R., and Palmer T. N., 1996: Interannual tropical rainfall variability in general circulation model simulations associated with the Atmospheric Model Intercomparison Project. *J. Climate.,* 9, 2727–2750.

Tao, S., and Chen L., 1987: A review of recent research on the East Asian summer monsoon in China. *Monsoon Meteorology,* C.-P. Chang and T. N. Krishnamurti, Eds., Oxford University Press, 60–92.

Wang, B., and LinHo , 2002: Rainy season of the Asian–Pacific summer monsoon. *J. Climate.,* 15, 386–398.

Warren, B. A., 1987: Ancient and medieval records of the monsoon winds and currents of the Indian Ocean. *Monsoons,* J. S. Fein and P. L. Stephens, Eds., John Wiley & Sons, 137–158.

Webster, P. J., 1987: The elementary monsoon. *Monsoons,* J. S. Fein and P. L. Stephens, Eds., John Wiley & Sons, 3–32.

Webster, P. J., Magana V. O., Palmer T. N., Shukla J., Tomas R. A., Yanai M., and Yasunari T., 1998: Monsoons: Processes, predictability, and the prospects for prediction. *J. Geophys. Res.,* 103, 14451–14510.

Wu, R., and Wang B., 2000: Interannual variability of summer onset over the western North Pacific and the underlying processes. *J. Climate.,* 13, 2483–2501.

Xie, P., and Arkin P. A., 1997: Global precipitation: A 17-year monthly analysis based on gauge observations, satellite estimates, and numerical model outputs. *Bull. Amer. Meteor. Soc.,* 78, 2539–2558.

Xie, P., and Arkin P. A., 1998: Global monthly precipitation estimates from satellite-observed outgoing longwave radiation. *J. Climate.,* 11, 137–164.

Zeng, X., 1999: The relationship between precipitation, cloud-top temperature, and precipitable water over the Tropics. *J. Climate.,* 12, 2503–2514.

Zhou, J.-Y., and Lau K. M., 1998: Does a monsoon climate exist over South America?. *J. Climate.,* 11, 1020–1040.

APPENDIX B

UNDERSTANDING DIFFERENT PRECIPITATION SEASONALITY REGIMES FROM WATER VAPOR AND TEMPERATURE FIELDS: CASE STUDIES

ER LU and XUBIN ZENG

Department of Atmospheric Sciences
The University of Arizona
Tucson, Arizona

Published in

Geographic Research Letters

2005, Volume 32, doi:10.1029/2005GL024333

B.1 Abstract

Different precipitation seasonality regimes, although produced by different surface and atmospheric conditions, can be understood from the basic atmospheric fields. By comparing the change of water vapor from winter to summer with the change of temperature using the North American Regional Reanalysis, three seasonality cases over the United States and Mexico are analyzed. In the western coast of the U.S., the change of temperature from winter to summer is much greater than the change of water vapor. So, relative to summer, the coldness of the winter air is much more significant than the dryness, which makes the winter have a large saturation extent and thus precipitation. In contrast, over South Mexico, the much more significant moistness of the summer air than its warmness is important to the summer monsoon precipitation. In the southeastern U.S. where precipitation occurs throughout the year, the changes of water vapor and temperature are roughly equivalent.

B.2 Introduction

The precipitation seasonality and its spatial difference is a fundamental issue of the climate, and has been studied over a century through analyzing the precipitations from observational records and model outputs with various statistical techniques [e.g., *Greely* 1893; *Henry* 1897; *Horn and Bryson* 1960; *Hsu and Wallace* 1976; *Walsh et al*. 1982; *Kirkyla and Hameed* 1989; *Finkelstein and Truppi* 1991]. The formation of precipitation is affected by complex dynamic and thermodynamic conditions (e.g., the surface characteristics and the atmospheric circulations), and, in different seasons and locations, these conditions can vary greatly. In this study, we attempt to provide an understanding of the different precipitation seasonality regimes in a unified manner from the basic atmospheric fields, instead of analyzing their specific surface and circulation characteristics though they are important, since, at a seasonal scale, the different dynamic and thermodynamic factors influencing the precipitation can be reflected in the atmospheric states.

Water vapor is required for precipitation; however, in some areas (e.g., the western coast of the U.S.), the largest precipitation of the year occurs when the water vapor is the least, and contrarily when water vapor is the largest, there is almost no precipitation. Our analysis indicates that the air temperature is the key to this case. *Bretherton et al*. [2004] also pointed out that the monthly mean precipitation over the tropical oceans can be well determined from the water vapor and temperature fields. The

comparative strengths of water vapor and temperature in winter and summer are analyzed in this study for the three major precipitation seasonality regimes over the continental United States and Mexico (US-Mexico).

B.3 Data

The daily precipitation analysis used in section B.4 is created by the Climate Prediction Center (CPC) of the National Oceanic and Atmospheric Administration and available at http://www.cpc.ncep.noaa.gov/products/precip/realtime/retro.html. The dataset starts from 1948 and covers the US-Mexico with 1°×1° horizontal resolution. More description of the data can be found in *Higgins et al*. [1999]. The daily precipitable water analysis used for making a comparison with precipitation is taken from the NASA Water Vapor Project [*Randel et al*. 1996], and is currently available for 12 years (1988-1999). The specific humidity, temperature, and precipitation used in section B.5 are taken from the North American Regional Reanalysis (NARR), which was developed by the National Centers for Environmental Prediction and is available at http://wwwt.emc.ncep.noaa.gov/mmb/rreanl/index.html. The dataset includes 25 years (1979-2003) and has resolutions of 3 hours in time, 32km in horizontal, and 29 layers in vertical. *Mesinger et al*. [2005] presented a detailed introduction and reliability evaluation of the data.

B.4 Precipitation Seasonality Cases

The precipitation seasonality can be classified as numerous regimes depending on the given standards, and, even in the United States, can be divided into six regimes as suggested by *Boyle* [1998]. For simplicity, in this study, we will focus on the three major precipitation seasonality regimes, which, though have already been known in *Hsu and Wallace* [1976], *Finkelstein and Truppi* [1991], and many others, are illustrated here. Figure B.1 is the standard deviation of the ten-year (1988-97) averaged annual time series of the daily precipitation analysis in the US-Mexico, which is useful in locating the strong precipitation seasonality areas. The maximal precipitation variations within a year are over the western coast of the U.S. (WC), South Mexico (SM), and the southeastern U.S. (SE). Figure B.2 shows the ten-year (1988-97) averaged annual cycles of the precipitation and precipitable water analyses at the centers of these maximal variations: 123°W/46°N in WC, 105°W/21°N in SM, and 90°W/33°N in SE. For convenience, these three centers will be denoted hereafter by WC, SM, and SE, respectively. The precipitations in WC (Fig. B.2a) and SM (Fig. B.2b) both have strong seasonal variations, but the former decreases from winter to summer, while the latter increases from winter to summer. The precipitation in SE can occur throughout the year (Fig. B.2c), but is dominated by the day-to-day variation, and the seasonal change is rather weak. Since the monthly mean precipitations of February and August can reflect the major difference of the precipitations between winter and summer in all the three regimes as shown in Fig. B.2, they will be used in this study to represent the winter and summer precipitations. The precipitable water, in contrast, exhibits the same seasonal pattern in the three regimes

(Fig. B.2). The relation between precipitation and precipitable water is examined in our follow-up study, and it is shown analytically that the precipitable water over the continent is dominated by the large seasonal change of the surface temperature, thus always increases from winter to summer.

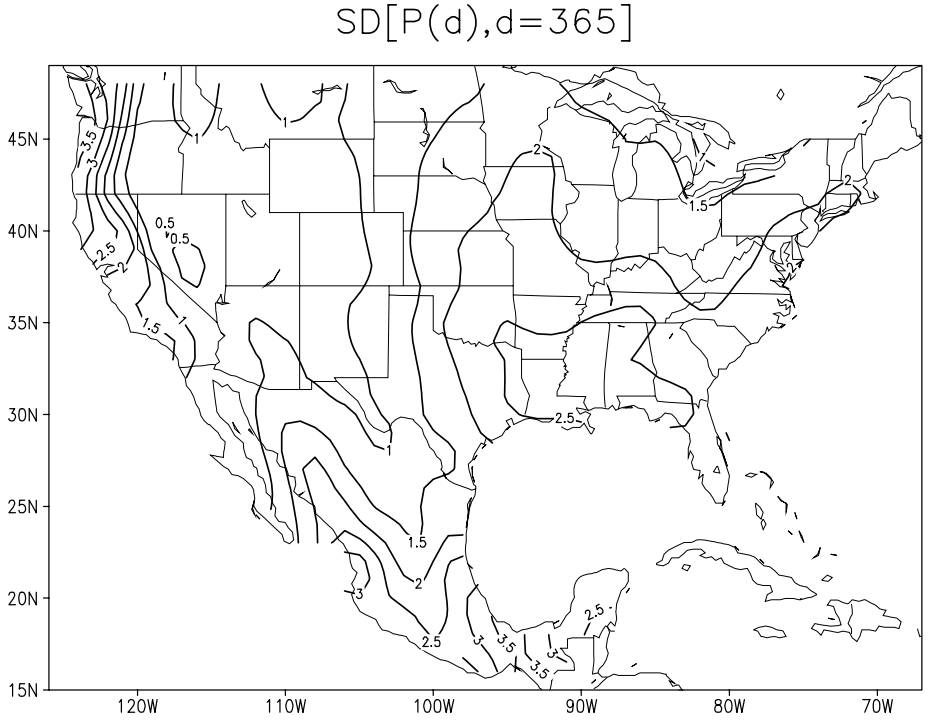

Figure B.1: Standard deviation of ten-year (1988-97) averaged annual time series of daily precipitation analysis. Unit is mm/day.

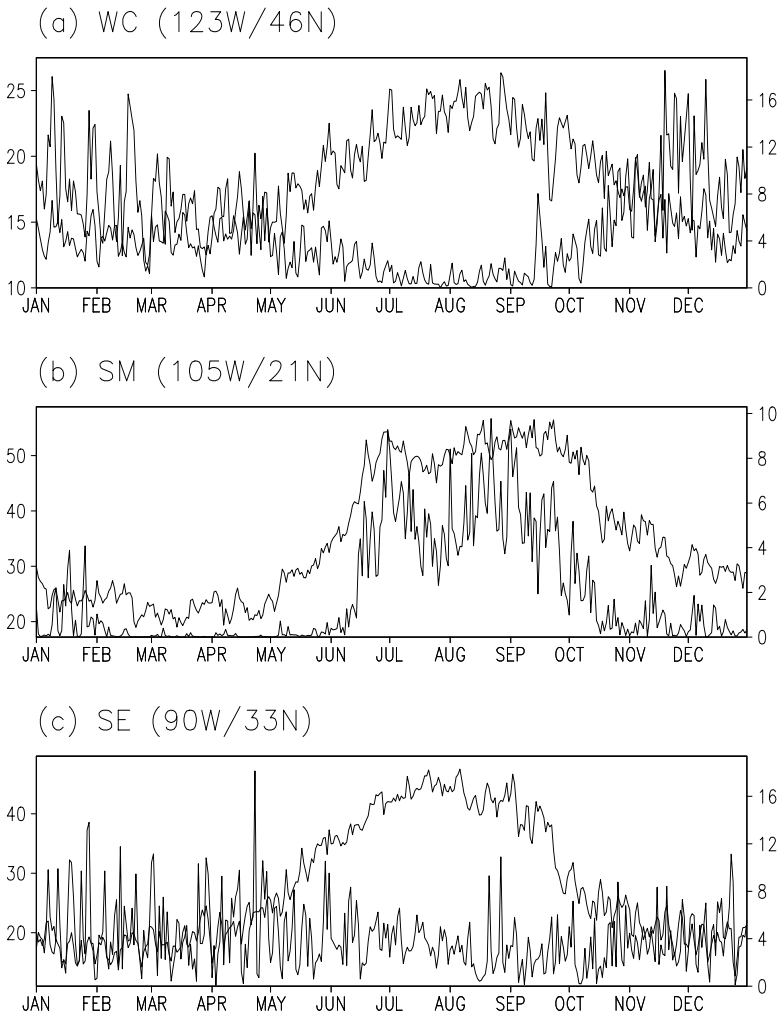

Figure B.2: Ten-year (1988-97) averaged daily analysis of precipitation (thick, right axis, unit: mm/day) and precipitable water (thin, left axis, unit: mm) at (a) WC; (b) SM; and (c) SE.

B.5 Understanding from Water Vapor and Temperature Fields

For a single precipitation process, the saturation of the water vapor in a layer or layers of the atmosphere is a critical condition for the formation of precipitation. At the seasonal or monthly timescale, should an overall higher saturation of the atmosphere correspond, to a great extent, to a larger precipitation? Generally, during the period studied (e.g., one month), if the total raining time is long (short), a large (small) precipitation and a large (small) mean saturation extent can both be expected, so the precipitation and the mean saturation extent of the period should be well positively correlated. *Bretherton et al*. [2004] found that the monthly mean precipitation over the tropical oceans can be well represented by the relative humidity calculated from the monthly mean precipitable water and the water vapor capacity of the atmosphere. Figures B.3a-c show the profiles of the 25-year averaged monthly mean relative humidity in February and August of the three regimes. In WC, the saturation extent in the rainy February is much greater than in the dry August at most of the levels (Fig. B.3a), and in SM, the saturation extent in the rainy August is much greater than in the dry February at all levels (Fig. B.3b). In SE, corresponding to the year-round precipitation, the saturation extent overall does not change much, and maintains a moderate level (Fig. B.3c). So, for the three seasonality regimes, the seasonal changes of the saturation extent from winter to summer are well consistent with the changes of the precipitation.

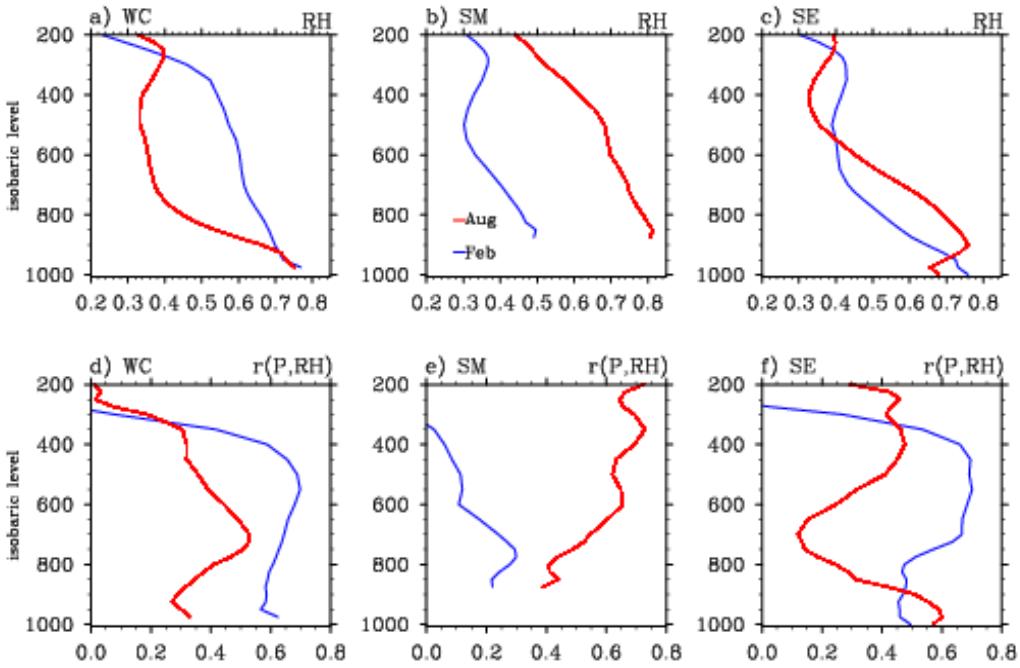

Figure B.3: Profiles of (a-c) relative humidity calculated from the 25-year (1979-2003) averaged monthly mean specific humidity and temperature; and (d-f) correlation between the 25-year time series of the monthly mean relative humidity and precipitation in February (blue) and August (red) at WC, SM, and SE.

Figures B.3d-f further provide the profiles of the correlation between the monthly mean relative humidity at a height and the monthly mean precipitation in February and August for the 25 years. The correlations are positive at almost all levels of the two months in the three regimes, and greater than 0.4 (i.e., the correlation at a 95% significance level) in most levels of all the rainy months (Fig. B.3d-f). The correlation of the dry August in WC is also significant at the middle levels (Fig. B.3d). These results imply that the monthly mean saturation extent can not only well reflect the seasonal tendency (increase, decrease, or no much change) of the monthly mean precipitation, but also indicate to a great extent the interannual variation of the monthly mean precipitation. Therefore, we can use the saturation extent to represent the precipitation in the following analysis. The correlation in the dry February of SM is small (Fig. B.3e), because the precipitation of the dry month only falls in a small portion of the time with a high relative humidity, but the monthly mean relative humidity can be influenced by the most part of the month that has no precipitation. To ensure the saturation extent can well reflect the changes of precipitation in those weak seasonality regimes, a pentad mean or running mean maybe more suitable.

The relative humidity is a function of water vapor and temperature, so the seasonal change of the precipitation can be evaluated from water vapor and temperature fields. Figure B.4 presents the profiles of the 25-year averaged monthly mean specific humidity and temperature in February and August for the three seasonality regimes. Note that the water vapor and temperature both increase from winter to summer at all levels and for all the three regimes. However, since they are different variables, it is difficult to

identify, from Fig. B.4, which increases more significantly from winter to summer and contributes more to the seasonal change of precipitation. So, we need an approach to measure the seasonal changes of the two variables. Here, an analytical method is used.

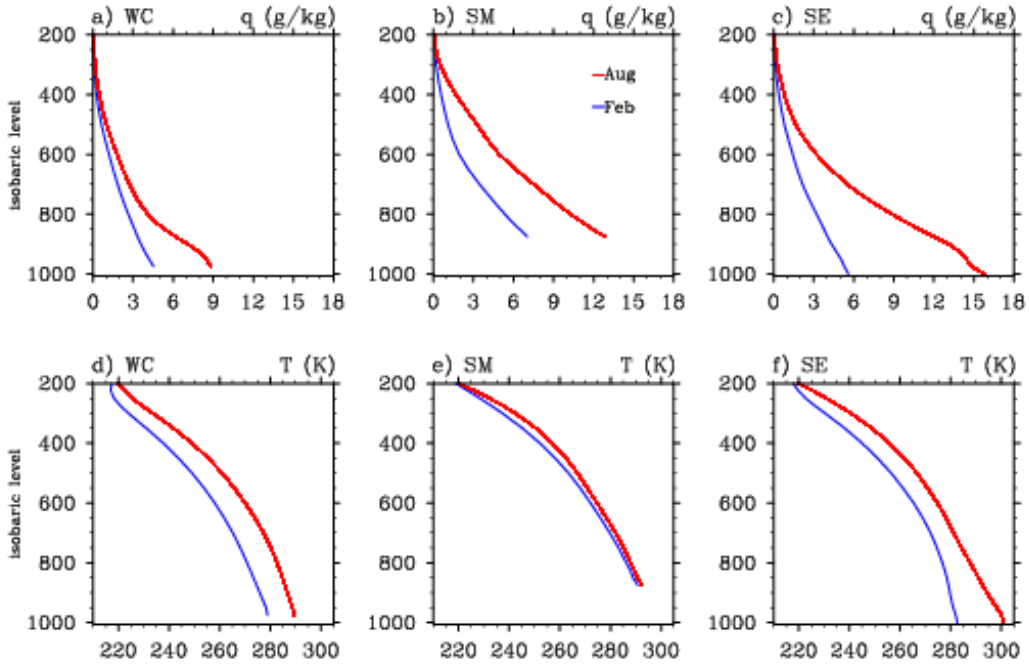

Figure B.4: Profiles of the 25-year averaged monthly mean (a-c) specific humidity (unit: g/kg) and (d-f) temperature (unit: K) in February (blue) and August (red) at WC, SM, and SE.

The change of the saturation extent, indicated by relative humidity (RH), from winter (win) to summer (sum) can be represented by $C_{sat} \equiv RH^{sum} / RH^{win}$. Using the definition of relative humidity $RH = e / e_s(T)$, where e is vapor pressure and $e_s(T)$ is the saturation vapor pressure at temperature T, it can be written as $C_{sat} = C_{vap} / C_{tem}$, where

$$C_{vap} \equiv e^{sum} / e^{win} \tag{B1}$$

and

$$C_{tem} \equiv e_s(T^{sum}) / e_s(T^{win}) \tag{B2}$$

are defined as the change of water vapor and the change of temperature, respectively, from winter to summer. If $C_{vap} = C_{tem}$, that is, the change of water vapor from winter to summer is equivalent to the change of temperature, then $C_{sat} = 1$, which means the saturation extent does not change from winter to summer, and, based on the consistence of the seasonal changes of precipitation and saturation extent from winter to summer, it can be inferred that the precipitation does not change much from winter to summer. When the change of water vapor from winter to summer is greater than the change of temperature ($C_{vap} > C_{tem}$), the saturation extent and precipitation increase from winter to summer ($C_{sat} > 1$). When the change of temperature is greater ($C_{tem} > C_{vap}$), the saturation extent and precipitation decrease ($C_{sat} < 1$). Using the expression of specific

humidity $q = \varepsilon e / p$, where p is pressure and ε the ratio of the gas constants for dry air and water vapor, then C_{vap} can be written as $C_{vap} = q^{sum} / q^{win}$ for the change at a pressure surface.

To better understand the meaning of C_{vap} and C_{tem}, (B1) and (B2) can be rewritten by defining the dew point temperature T_d through $e \equiv e_s(T_d)$ and expressing the saturation vapor pressure as $e_s(T) = A\exp(-L/R_v T)$ (the integrated form of the Clausius-Clapeyron equation), in which R_V is the gas constant for water vapor, L the latent heat of vaporization, and A the integration constant. Then, (B1) and (B2) become

$$C_{vap} = \exp[a(T_d^{sum} - T_d^{win})], \tag{B3}$$

and

$$C_{tem} = \exp[b(T^{sum} - T^{win})], \tag{B4}$$

where $a = L/(R_v T_d^{sum} T_d^{win})$ and $b = L/(R_v T^{sum} T^{win})$ vary little with temperature and dew point within their normal ranges, and can be taken as constants. So, C_{vap} and C_{tem} can reflect the differences of dew point and temperature, respectively, between winter and summer. The C_{sat} can be written as

$$C_{sat} = \exp[a(T_d^{sum} - T_d^{win}) - b(T^{sum} - T^{win})]. \tag{B5}$$

It shows how the differences of dew point and temperature contribute to the change of saturation extent.

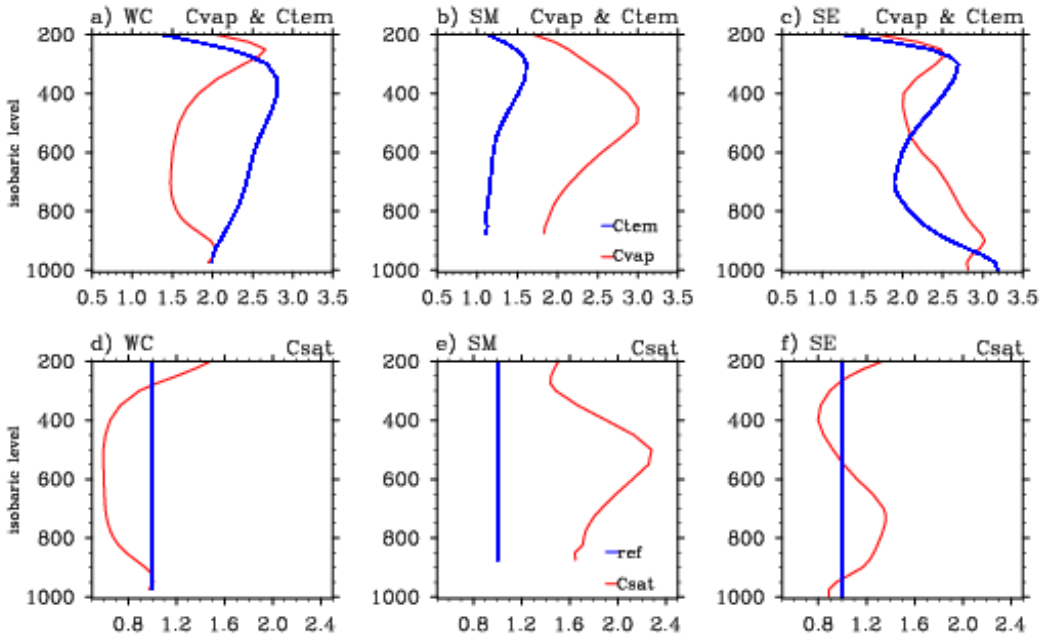

Figure B.5: Profiles of (a-c) the change of water vapor (C_{vap}, red) and the change of temperature (C_{tem}, blue) calculated from the 25-year averaged monthly mean specific humidity and temperature of February and August; and (d-f) the change of saturation extent (C_{sat}, red) and a reference line of 1.0 (blue) at WC, SM, and SE.

Figures B.5a-c present the profiles of C_{vap} and C_{tem} calculated with the 25-year averaged monthly mean data of February and August for the three regimes. In WC (Fig. B.5a), the change of temperature (C_{tem}) is much greater than the change of water vapor (C_{vap}) in the layer from 900 to 300hPa. This means that, relatively, the winter atmosphere over WC is cold but not so dry, and the summer atmosphere is warm but not so moist. Therefore, the winter has a higher relative humidity and becomes the rainy season of the year, while the summer has a lower relative humidity with little precipitation. In this interesting precipitation seasonality regime shown in Figs. B.2a and B.4a, when the water vapor (e, q, or precipitable water) is the least of the year in winter, the precipitation is the largest, while when the water vapor is the largest in summer, the precipitation is the least. So, the effect of the temperature is the key to the opposite seasonal behaviors of the water vapor and the precipitation. In SM (Fig. B.5b), the change of water vapor (C_{vap}) from winter to summer is much greater than the change of temperature (C_{tem}) in all levels, especially in the middle layer (500hPa). This implies that, relatively, the winter is dry but not so cold (the temperature is actually very close to that of summer), which makes the winter saturation and precipitation very small. The summer is rather moist but not particularly hot, so the atmosphere is easy to saturate, and the huge summer monsoon precipitation forms. The averaged relative humidity in summer is greater than 45% at all levels and can reach 80% at the lowest level (Fig. B.3b). In SE, where precipitation occurs throughout the year, the changes of water vapor and temperature from winter to summer are roughly equivalent (Fig. B.5c). The configuration of the profiles of C_{vap} and

C_{tem} is kind of a combination of the above two cases. A careful examination of the changes of water vapor and temperature in the upper and lower levels may need a pentad or running mean for the data. The profiles of C_{sat} in Figs. B.5d-f illustrate the significance of the change of water vapor from winter to summer comparative with the change of temperature with aid of the reference line of $C_{sat} = 1$.

B.6 Summary

The precipitation seasonality can vary from place to place across the world. In this study, the three major precipitation seasonality regimes over the US-Mexico are understood from the comparative strengths of the water vapor and temperature in winter and summer. Our analysis suggests that, when understanding the precipitation seasonality, especially the regime with a negative correlation between the precipitation and water vapor as shown in Fig. B.2a, the effect of temperature, in addition to water vapor, should be taken into account. The water vapor, described by e, q, or precipitable water, and temperature both increase from winter to summer (Figs. B.2 and B.4). The key here is how to measure and compare the changes of the different variables of water vapor and temperature. For this purpose, two dimensionless numbers, C_{vap} and C_{tem}, are defined in this study.

In WC where winter is the rainy season, the change of temperature (C_{tem}) from winter to summer is much greater than the change of water vapor (C_{vap}), suggesting that

the winter air is cold but not so dry and the summer air is warm but not so moist. So, the saturation extent and precipitation are larger in winter and smaller in summer. In SM where summer is the rainy season, the change of water vapor (C_{vap}) is much greater than the change of temperature (C_{tem}), which means the winter air is dry but not so cold and the summer air is moist but not that hot. So, the saturation and precipitation are smaller in winter but larger in summer. In SE, where precipitation prevails the entire year, the changes of water vapor and temperature from winter to summer are overall equivalent. To better compare the changes of water vapor and temperature in the weak precipitation seasonality regimes, a pentad mean or running mean maybe more suitable.

It should be noted that, for precipitation, water vapor and temperature are not the cause, but an atmospheric condition. In different places and seasons, the precipitation may be affected by different surface conditions and different dynamic and thermodynamic processes involved in the atmosphere. However, at the seasonal scale, all the physical factors influencing the precipitation can be reflected in the water vapor and temperature fields, which makes it possible for us to understand the different precipitation seasonality regimes through them. The dynamic analysis of the rainy season precipitation of the three regimes, e.g., their dominant atmospheric circulations and systems, will be presented separately.

B.7 Acknowledgments

This work was supported by NOAA under grant NA05OAR4310008 and NASA under grant NNG04GL25G. The North American Regional Reanalysis, precipitation analysis, and precipitable water analysis are distributed by the NCEP/EMC, the NCEP/CPC, and the NASA/DAAC, respectively.

B.8 References

Boyle, J. S. (1998), Evaluation of the annual cycle of precipitation over the United States in GCMs: AMIP simulations, *J. Clim.*, *11*, 1041–1055.

Bretherton, C. S., M. E. Peters, and L. E. Back (2004), Relationships between water vapor path and precipitation over the tropical oceans, *J. Clim.*, *17*, 1517–1528.

Finkelstein, P. L., and L. E. Truppi (1991), Spatial distribution of precipitation seasonality in the United States, *J. Clim.*, *4*, 373–385.

Greely, A. W. (1893), Rainfall types of the United States, *Natl. Geogr. Mag.*, *5*, 45-58.

Henry, A. J. (1897), Rainfall of the United States, with annual, seasonal, and other charts, *U. S. Weather Bureau Bull. D.*, 11-13.

Higgins, R. W., Y. Chen, and A. V. Douglas (1999), Interannual variability of the North American warm season precipitation regime, *J. Clim.*, *12*, 653–680.

Horn, L. H., and R. A. Bryson (1960), Harmonic analysis of the annual march of precipitation over the United States, *Ann. Assoc. Amer. Geogr.*, *50*, 157–171.

Hsu, C.-P., and J. M. Wallace (1976), The global distribution of the annual and semiannual cycles in precipitation, *Mon. Wea. Rev.*, *104*, 1093–1101.

Kirkyla, K. I., and S. Hameed (1989), Harmonic analysis of the seasonal cycle in precipitation over the United States: A comparison between observations and a general circulation model, *J. Clim.*, *2*, 1463–1475.

Mesinger, F., et al. (2005), North American Regional Reanalysis, *Bull. Amer. Meteor. Soc.*, submitted.

Randel, D. L., T. J. Greenwald, T. H. V. Haar, et al. (1996), A new global water vapor dataset, *Bull. Amer. Meteor. Soc., 77*, 1233–1254.

Walsh, J. E., M. B. Richman, and D. W. Allen (1982), Spatial coherence of monthly precipitation in the United States, *Mon. Wea. Rev.*, *110*, 272–286.

APPENDIX C

CHANGE OF PRECIPITABLE WATER CORRESPONDING TO SURFACE TEMPERATURE INCREASE OF VARYING SCALE: THEORETICAL ANALYSES

ER LU and XUBIN ZENG

Department of Atmospheric Sciences
The University of Arizona
Tucson, Arizona

Submitted for publication in

Geographic Research Letters

September 2005

C.1 Abstract

Water vapor plays a crucial role in the climate system, and how the precipitable water (W) changes is an important issue. The change of W corresponding to surface temperature increase of varying scale is analyzed theoretically. When the surface temperature change is small, the changes of W and surface temperature are weakly correlated. However, when the surface temperature change becomes large, as in seasonal changes of mid-high latitudes, the changes of W and surface temperature, dominated by the significant thermodynamic effect, can be strongly correlated. The seasonal W is prescribed in previous research from the surface temperature for the global oceans. Our theoretical study explains why the seasonal W can be prescribed from the surface temperature, and further indicates that the prescription can be carried out over both oceans and lands, but only for the mid-high latitudes, not the tropics.

C.2 Introduction

The atmospheric water vapor, as both a greenhouse gas and a hydrological component, plays a crucial role in the climate system by influencing the radiation and energy balance of the atmosphere and the earth's surface. The total water vapor in the atmospheric column, or the precipitable water (W), can be observed from satellites and radiosondes [e.g., *Randel et al*., 1996; *O'Sullivan et al*., 2000], and can be both assimilated into and output from atmospheric models [e.g., *Filiberti et al*., 1994; *Mesinger et al*., 2005], thus has become a conventional meteorological variable. The tempo-spatial variations of the W at different scales and their dominant factors are of a great concern to the hydro-climate community. The purpose of this study is to provide theoretical analyses of the changes of W corresponding to a surface temperature increase of varying scale.

The W is controlled by both the thermodynamic condition (e.g., the surface temperature) and the dynamic condition (e.g., the large-scale circulations). However, *Stephens* [1990] revealed that, at seasonal scale, the W can be prescribed only from the surface temperature, since the effect of large-scale motion is small. His study was for the global oceans and did not include the lands. His results also indicate that the seasonal W and surface temperature are well correlated only over the mid-high latitude regions, and the correlations for the tropic regions are weak. In this study, we will theoretically prove that the seasonal W can be prescribed from the surface temperature, not only over oceans

but also over lands, however, only for the mid-high latitudes, not the tropics. A general relation linking the changes of W, surface temperature, and surface relative humidity is derived, and the mechanisms involved in the changes of W corresponding to small and large surface temperature changes are analyzed.

C.3 Relations from Data

It is found from observed data and model output (e.g., the North American Regional Reanalysis [*Mesinger et al.*, 2005]) that, corresponding to small surface temperature increases, W can both increase and decrease, so the changes of W and surface temperature are in general not closely correlated (figure not shown). Here an example of the seasonal pattern of W over the land of mid-high latitudes is presented. By using the ten-year (1988-97) daily analyses of W and precipitation at a 1°×1° resolution over the continental United States and Mexico (US-Mexico), obtained respectively from the NASA Water Vapor Project [*Randel et al*., 1996] and the Climate Prediction Center of NOAA [*Higgins et al*., 1999], the annual cycles of the W and precipitation are contrasted in Fig. C.1 at the locations of 123°W/46°N in the western coast of the U.S. (WC), 105°W/21°N in South Mexico (SM), and 90°W/33°N in the southeastern U.S. (SE), which are the centers of the maximal standard deviation of the averaged daily precipitation over the US-Mexico (Fig. B.1 in Appendix B). The different annual cycles of the precipitation in Fig. C.1, representing the three major seasonality regimes over the US-Mexico, have been understood from water vapor and temperature fields in *Lu and*

Zeng [2005]. Since W has been used to determine the monsoon onset and retreat dates [e.g., *Zeng and Lu*, 2004; *Li and Chen*, 2005], the comparisons of the W and precipitation at both synoptic and seasonal scales are required to ensure the reliability of the methods, which will be analyzed in our further work. The W at the three locations, in contrast, shows the same seasonal pattern of having an increase from winter to summer (Fig. C.1).

Figure C.2 is the distribution of the correlation between the W at a point in the central U.S. (100°W, 40°N) and the entire W field over the US-Mexico. The contour of 0.95 almost exactly follows the eastern and southern U.S. coasts, while the contour of 0.9 largely follows the western coast. The coefficients over Mexico and some ocean areas near the continent are all above 0.8. These indicate that the seasonal W has a high spatial coherence over the US-Mexico. It can be inferred from the annual cycles of W in Fig. C.1 that W increases from winter to summer over each grid box of the US-Mexico. Similarly, the W over other lands of mid-high latitudes also wholly increases from winter to summer (figures not shown).

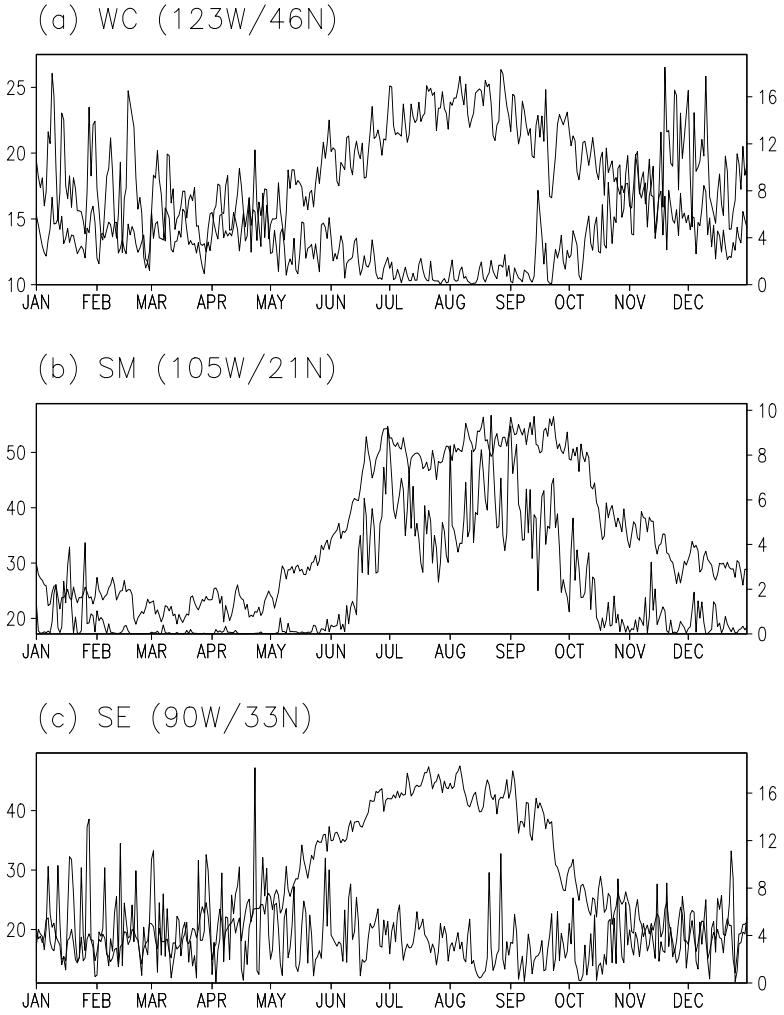

Figure C.1: Ten-year (1988-97) averaged daily analysis of precipitable water (thin, left axis, unit: mm) and precipitation (thick, right axis, unit: mm/day) at (a) WC, (b) SM, and (c) SE.

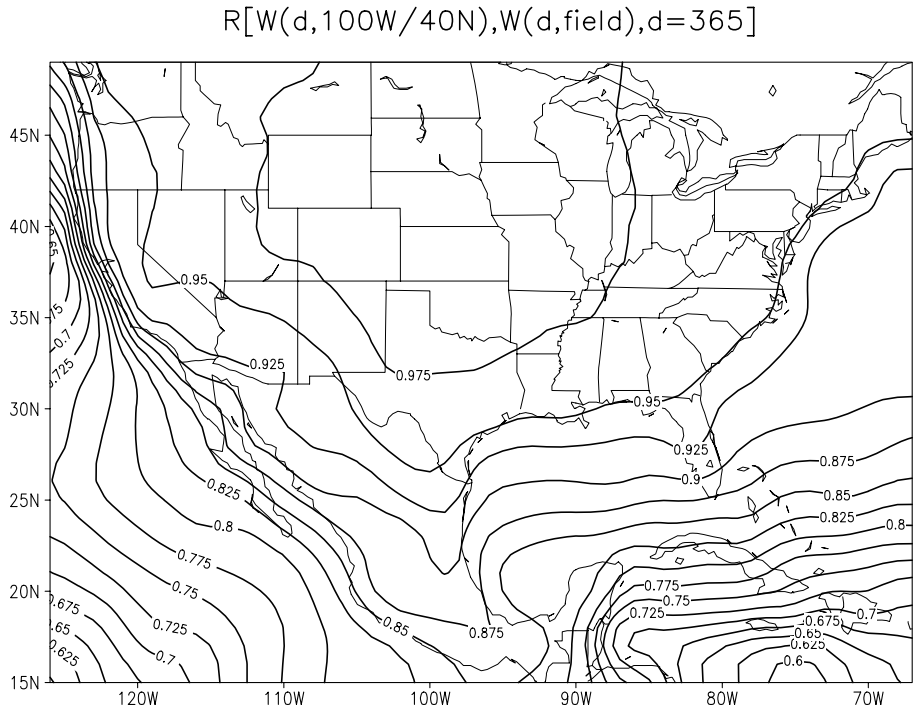

Figure C.2: Distribution of correlation coefficient between the ten-year (1988-97) averaged time series of daily W analysis at (100°W, 40°N) and those over the entire field.

C.4 Theoretical Analyses

The W can be expressed as

$$W = \int_0^{p_s} q \frac{dp}{g}, \tag{C1}$$

where q is specific humidity, p pressure, p_s surface pressure, and g gravitational acceleration. Using the sigma coordinate $\sigma \equiv p/p_S$ and the expression of specific humidity $q = \varepsilon e/p$, (C1) can be rewritten as

$$W = \varepsilon \int_{\sigma=0}^{\sigma=1} e \frac{d(\ln \sigma)}{g}, \tag{C2}$$

where e is vapor pressure and ε the ratio of the gas constants for dry air and water vapor. For an atmospheric process from state 1 to state 2, the difference of W can be calculated as

$$\Delta W = \varepsilon \int_{\sigma=0}^{\sigma=1} (e_2 - e_1) \frac{d(\ln \sigma)}{g}. \tag{C3}$$

With the definition of relative humidity $RH = e/e_s(T)$, (C3) can be expressed as

$$\Delta W = \varepsilon \int_{\sigma=0}^{\sigma=1} e_1 C_{sat} (C_{tem} - \frac{1}{C_{sat}}) \frac{d(\ln \sigma)}{g}, \tag{C4}$$

where $C_{tem} \equiv e_s(T_2)/e_s(T_1)$ and $C_{sat} \equiv RH_2/RH_1$ are defined as the change of temperature and the change of saturation extent, respectively, from state 1 to state 2 as in

Lu and Zeng [2005]. Equation (C4) indicates that at a specific height σ, whether the contribution to ΔW is positive or not is determined by the sign of $(C_{tem} - 1/C_{sat})$.

For seasonal changes or synoptic processes with no strong convections, the vapor pressure e is maximal at the surface, and decreases exponentially with height [*Peixoto and Oort*, 1992], which makes it possible to calculate the W using only the surface vapor pressure, instead of the vertical integration in (C2). Actually, it has been revealed that the monthly mean surface dew point temperature has an extremely high correlation with the W [e.g., *Reitan*, 1963; *Viswanadham*, 1981]. It can be inferred that normally the difference of the vapor pressure between the two states, Δe, also decreases with height, so the vertical integration in (C3), and then (C4), can also be represented by the surface value of the integrated function. Therefore, (C4) can be expressed as

$$\Delta W = c[e_1 C_{sat}(C_{tem} - 1/C_{sat})]_{\sigma=1} \propto \Delta_{RH_s}^{T_s}, \tag{C5}$$

where c is the coefficient and can be determined from data, $\Delta_{RH_s}^{T_s} \equiv (C_{tem} - 1/C_{sat})_{\sigma=1}$ determines the sign of ΔW, in which T_s and RH_s represent the surface temperature and relative humidity. Using the analytical expression of saturation vapor pressure $e_s(T) = A\exp(-L/R_v T)$, where T, R_V, L, and A are air temperature, the gas constant for water vapor, the latent heat of vaporization, and a constant, respectively, we obtain $C_{tem} = a^{\Delta T}$, where $\Delta T = T_2 - T_1$ and $a = \exp[L/(R_v T_1 T_2)]$. Assuming

$(T_1, T_2) \in [-30, 40]^\circ C$ for the surface atmosphere, a is calculated to vary from 1.056 to 1.095, and hence can be taken as a constant of 1.08. So, the expression of $\Delta_{RH_s}^{T_s}$ becomes

$$\Delta_{RH_s}^{T_s} = 1.08^{\Delta T_s} - RH_{s1}/RH_{s2} \ . \tag{C6}$$

For an isolated atmospheric column that has no water vapor exchange with the surface and the surrounding air ($\Delta W = 0$), the changes of the surface temperature and relative humidity of the two states satisfy the equation $1.08^{\Delta T_s} - RH_{s1}/RH_{s2} = 0$. Figure C.3 presents the contours of the ΔT_s as a function of RH_{s1} and RH_{s2} obtained from this equation. The real atmosphere, however, is an open system, in which water vapor can exchange with the outside ($\Delta W \neq 0$). For a specific ΔT_s, the RH_{s1} and RH_{s2} in the domain above (below) the contour of ΔT_s in Fig. C.3 make $\Delta W > 0$ ($\Delta W < 0$), indicating an increase (decrease) of W from state 1 to state 2.

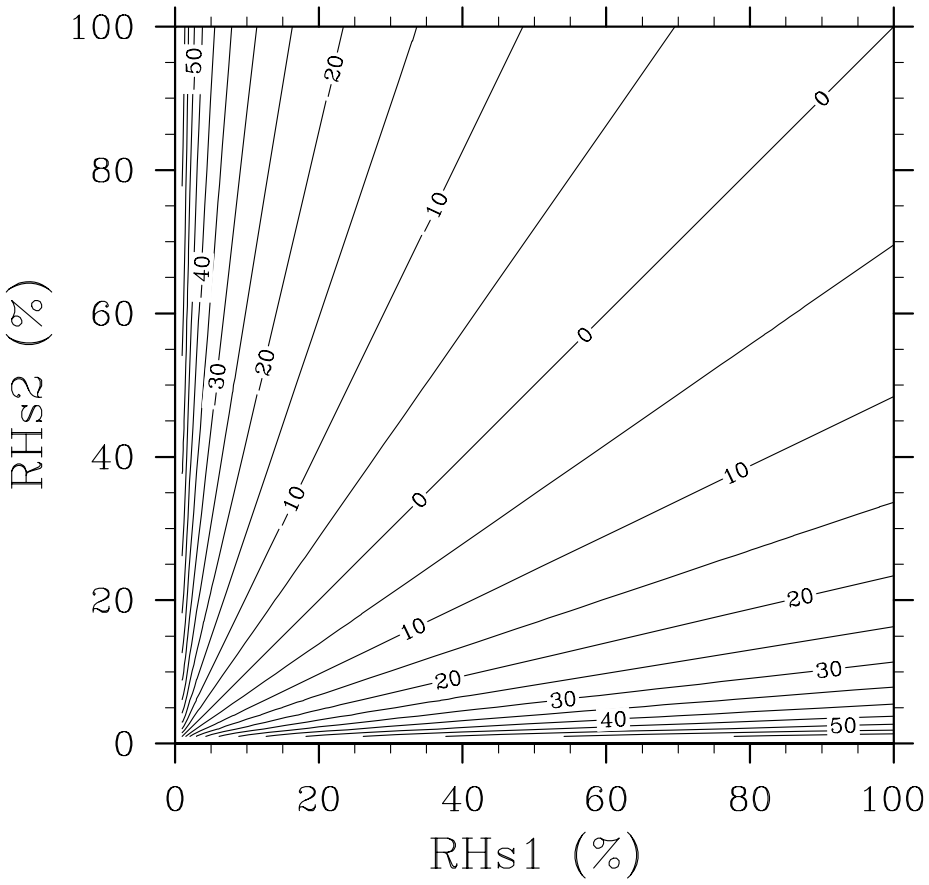

Figure C.3: Contours of ΔT_s as a function of RH_{s1} and RH_{s2} for an isolated atmospheric column ($1.08^{\Delta T_s} - RH_{s1}/RH_{s2} = 0$).

Suppose the relative humidity RH_{s1} and RH_{s2} take values from 0 to 1 with an even possibility, then the areas of the domains above and below the contour of ΔT_s represent, respectively, the possibilities of having an increase and decrease of W, which can be expressed as

$$\Pr\big|_{\Delta W>0} = 1 - 0.5/1.08^{\Delta T_s} \tag{C7}$$

and

$$\Pr\big|_{\Delta W<0} = 0.5/1.08^{\Delta T_s} \ . \tag{C8}$$

The latter is also the value of RH_{s2} when the relative humidity changes from $RH_{s1} = 0.5$ in an isolated system ($\Delta W = 0$), or it can be denoted as

$$RH_{s2}\big|_{\Delta W=0}^{RH_{s1}=0.5} = 0.5/1.08^{\Delta T_s} \ . \tag{C9}$$

Figure C.4 shows the changes of the probabilities of having an increase and decrease of W with ΔT_s. The W has the same possibility to increase or decrease when there is no surface temperature change, and the possibility of having an increase (decrease) of W increases (decreases) rapidly with ΔT_s.

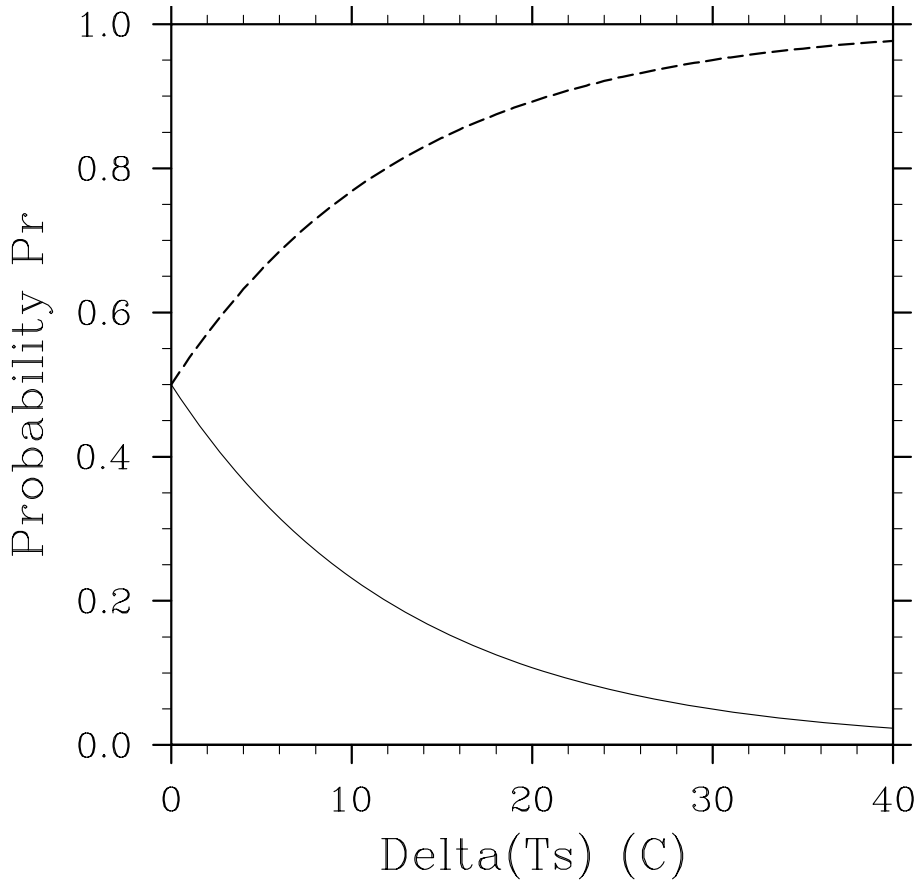

Figure C.4: Changes of the probabilities of having $\Delta W > 0$ ($\Pr|_{\Delta W>0}$, dashed) and $\Delta W < 0$ ($\Pr|_{\Delta W<0}$, solid) with ΔT_s.

We only need to consider the situation with surface temperature increase ($\Delta T_s > 0$). When ΔT_s is small, as in synoptic processes or the seasonal changes over tropics, the probability of having a decrease of W is just a little less than that of having an increase of W (Fig. C.4), and, in the two cases, RH_{s1} and RH_{s2} can both take the normal values (Fig. C.3). For example, assuming ΔT_s=3°C, the probabilities of having an increase and decrease of W are 0.60 and 0.40, respectively. Corresponding to an initial relative humidity (RH_{s1}) of 0.50, the final relative humidity (RH_{s2}) only needs to be greater than 0.40 to make W increase or less than 0.40 to make W decrease, and both cases are possible in reality. Therefore, when the surface temperature has a small increase, the W may increase or decrease, and the changes of W and surface temperature are weakly correlated.

When the surface temperature has a large increase, e.g., the seasonal changes of mid-high latitudes, especially over lands, the possibility of having a decrease of W from winter to summer becomes very small. Moreover, the summer relative humidity needs to become particularly small, which is rare in reality. For example, according to *Peixoto and Oort* [1992; Fig. 7.4c], the increase of the surface temperature from January to July is in the range of 20~35°C over most of the United States. With a winter relative humidity of 0.50, the summer relative humidity needs to be less than 0.04 ~ 0.12 to make the W decrease, and this is very difficult to satisfy [*Peixoto and Oort*, 1992]. Over most of Mexico, the increase of the surface temperature from January to July ranges within 5~15°C. To make W decrease, the summer relative humidity should be less than 0.17 ~

0.35 with the winter relative humidity of 0.50, and this is still difficult to satisfy. Therefore, the W over the land always increases from winter to summer, which explains the positive correlation between the seasonal W and surface temperature. It can be inferred that the seasonal W and surface temperature, since the interannual variabilities of their annual maximums and minimums are generally all small compared with their annual ranges, are well correlated. Note that, since the annual range of the surface temperature over ocean is usually much smaller than that over land due to the ocean's larger heat capacity, the tendency of the W with an increase from winter to summer is relatively weaker over ocean, which reduces sharply the correlation coefficients in Fig. C.2 over the tropical oceans, especially the northeast Pacific Ocean near California.

When studying the relationship between the monthly mean W and sea surface temperature (SST) from June 1979 to June 1983 averaged over seven regions of the global oceans, *Stephens* [1990] found in his Fig. 10 that the correlations between the monthly W and SST are weak for some of the regions but are very strong for the others. The explanation from the above theoretical analysis is that the weak correlations are all for the tropic regions where the annual range of the monthly SST is only 1~2°C as indicated in his figure, and the strong correlations are all for the mid-high latitude regions where the annual range of the monthly SST is 6~8°C. It was suggested in his study that the seasonal W over oceans can be prescribed from SST since the effects from the large-scale circulations are small. Since the annual range of the surface temperature of the lands of mid-high latitudes is generally much larger, the seasonal W and surface temperature should also be well correlated based on our above theoretical analysis.

Therefore, the seasonal W over lands, at least of mid-high latitudes, may also be prescribed from the surface temperature, and this will be investigated in our future work by using observational data and model output.

The W is controlled by both the thermodynamic condition (the surface and air temperatures) and the dynamic condition (the atmospheric circulations converging the water vapor). In the above analysis, the dynamic effect is implicitly included by the relative humidity. To highlight the dynamic effect, a W-based parameter, which actually reflects the change of relative humidity, was used by *Prabhakara et al.* [1979] and *Stephens* [1990]. The dynamic and thermodynamic effects involved in the change of W can be analyzed qualitatively from the atmospheric water vapor balance equation, $\partial W/\partial t = C + E - P$, where $C \equiv -\int_0^{p_s} \nabla \cdot (q\vec{V})\, dp/g$ is the water vapor convergence of the column, E the evaporation, and P the precipitation. Integrating the equation over the time period $[t_1, t_2]$ yields

$$\Delta W = \int_{t_1}^{t_2} (C + E - P) dt \,. \tag{C10}$$

We can assume, for simplicity, only dry time periods ($P = 0$) are included in the integration, since for rainy time ($P \neq 0$), the $C + E$ can more or less be offset by the P. When there is an increase in the surface temperature T_s, it can thermally induce an atmospheric circulation, which converges more water vapor and makes a contribution to the C, denoted by C_T. The remaining part, i.e., $C_D = C - C_T$, can then represent the dynamic effect of the atmosphere. Then, (C10) becomes

$$\Delta W = \int_{t_1}^{t_2} (C_T + C_D + E)dt \,. \qquad \text{(C11)}$$

The C_T should be determined by the surface temperature change rate, so can be expressed as $C_T = b\,dT_s/dt$, where b is a constant. Assuming the surface temperature increases ΔT_s during the time period, then (C11) can be written as

$$\Delta W = b\Delta T_s + (\overline{C_D} + \overline{E})\Delta t\,, \qquad \text{(C12)}$$

where $\overline{C_D}$ and $\overline{E}$ are the averages over the time period. When the surface temperature change is small, as in synoptic changes or seasonal changes over tropics, $b\Delta T_s$ is small, and the C_D can be a strong convergence or divergence. So, the W can increase or decrease due to the dynamic effect of the atmosphere. In contrast, when the surface temperature change is large, as in the seasonal changes over lands of mid-high latitudes, $b\Delta T_s$ and $\overline{E}$ are important terms, and $\overline{C_D}$ is smaller partly because C_D may offset itself during the long period. So, the W always increases from winter to summer, dominated by the thermodynamic effects.

C.5 Summary

The W is determined by the vertical profiles of temperature and relative humidity, but can be estimated by using only the surface temperature and relative humidity. The contributions of the changes in the surface temperature and relative humidity to the change of W are evaluated in this study, and the main results are summarized

schematically in Fig. C.5. When the surface temperature has a small increase (Fig. C.5a), as in synoptic processes or seasonal changes over tropics, its influence to the change of W may be offset by the change in the surface relative humidity. And W can increase or decrease through strong convergence or divergence of the water vapor. Therefore, the correlation between the changes of W and surface temperature is very weak. The atmospheric circulation converging or diverging the water vapor are mainly controlled by the dynamic effect of the atmosphere, and the thermodynamic effect is not important.

When the surface temperature increase becomes large (Fig. C.5b), as in seasonal changes of mid-high latitudes especially over land, its contribution to the change of W is so important that it is extremely hard to be offset through the normal fluctuations in the surface relative humidity, unless the surface relative humidity becomes incredibly small. In other words, relatively, the surface temperature has a larger seasonal change, but the seasonal change in surface relative humidity is smaller. So, the W always increases from winter to summer, and the seasonal W and surface temperature can be well correlated. This suggests that the seasonal W over lands of mid-high latitudes may also be prescribed from the surface temperature, which will be studied in our further work. The seasonal change of W is dominated by the thermodynamic effect. With the increase of the surface temperature, the water vapor-holding capability of the atmosphere is enhanced, and the thermally driven atmospheric circulations are strengthened, which converges more water vapor so the W keeps increasing in the seasonal process.

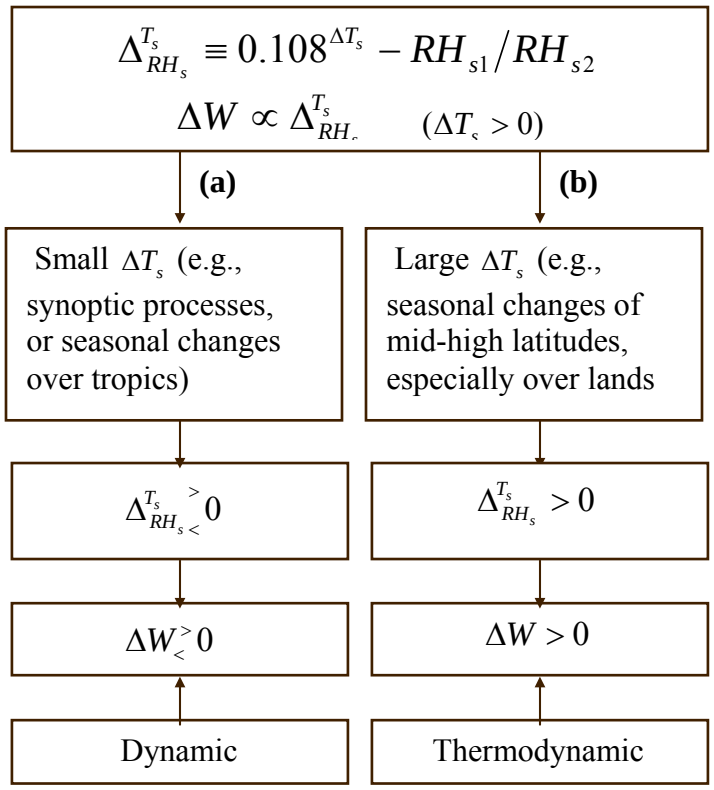

Figure C.5: A schematic of the changes of W corresponding to a (a) small and (b) large surface temperature increase, as well as the mechanisms involved in the changes.

C.6 Acknowledgments

This work was supported by NOAA under grants NA06GP0569 and NA16GP1619 and NASA under the EOS/IDS program (429-81-22). The precipitable water analysis, precipitation analysis, and NARR reanalysis are distributed by the NASA/DAAC, NCEP/CPC, and NCEP/EMC respectively.

C.7 References

Filiberti, M. A., L. Eymard, and B. Urban (1994), Assimilation of satellite precipitable water in a meteorological forecast model, *Mon. Weather Rev.*, *122*, 486–506.

Higgins, R. W., Y. Chen, and A. V. Douglas (1999), Interannual variability of the North American warm season precipitation regime, *J. Clim.*, *12*, 653–680.

Li, H., and B. Chen (2005), The evolution of precipitable water associated with the Asian and Australian monsoons as revealed from MODIS/SSMI, ECMWF and NCEP reanalysis data sets, *Geophys. Res. Lett.*, *32*, L10811, doi:10.1029/2005GL022570.

Lu, E., and X. Zeng (2005), Understanding different precipitation seasonality regimes from water vapor and temperature fields: Case studies, *Geophys. Res. Lett.*, *32*, doi:10.1029/2005GL024333.

Mesinger, F., et al. (2005), North American Regional Reanalysis, *Bull. Am. Meteorol. Soc.*, submitted.

O'Sullivan, D. B., B. M. Herman, D. Feng, D. E. Flittner, and D. M. Ward (2000), Retrieval of water vapor profiles from GPS/MET radio occultations, *Bull. Am. Meteorol. Soc.*, *81*, 1031–1040.

Peixoto, J. P. and A. H. Oort (1992), *Physics of Climate,* American Institute of Physics, 520 pp.

Prabhakara, C., G. Dalu, R. C. Lo, and N. R. Nath (1979), Remote sensing of seasonal distribution of precipitable water vapor over the oceans and the inference of boundary layer structure, *Mon. Weather Rev.*, *107*, 1388–1401.

Randel, D. L., T. J. Greenwald, T. H. V. Haar, et al. (1996), A new global water vapor dataset, *Bull. Am. Meteorol. Soc., 77*, 1233–1254.

Reitan, C. H. (1963), Surface dew point and water vapor aloft, *J. Appl. Meteor., 2*, 776–779.

Stephens, G. L. (1990), On the relationship between water vapor over the oceans and sea surface temperature, *J. Clim.*, *3*, 634–645.

Viswanadham, Y. (1981), The relationship between total precipitable water and surface dew point, *J. Appl. Meteor., 20*, 3–8.

Zeng, X., and E. Lu (2004), Globally unified monsoon onset and retreat indexes, *J. Clim*., *17*, 2241-2248.

APPENDIX D

A CLARIFICATION OF THE ISSUES IN THE GLOBALLY UNIFIED MONSOON INDEX

ER LU and XUBIN ZENG

Department of Atmospheric Sciences
The University of Arizona
Tucson, Arizona

Submitted for publication in

Journal of Climate

October 2005

D.1 Abstract

The globally unified monsoon index (GUMI) proposed by using precipitable water (W) in our earlier work has generated interests in the monsoon community. To ensure the reliability of the GUMI, three issues are clarified: (1) the rationality of using W to determine monsoon onset and retreat, (2) the inability of W to exactly identify the global monsoon regions, and (3) the rationality of the threshold taken in the criterion.

It is revealed that in monsoon regions, precipitation (P) has a larger increase from winter to summer, while in nonmonsoon regions, P decreases or does not change much. In contrast, the W always increases from winter to summer in both monsoon regions and some nonmonsoon regions since the annual range of temperature is large. So, distinguishing the global monsoon regions from nonmonsoon regions, although can be made by P, cannot be made by W. In monsoon regions, the W not only increases from winter to summer, but also reflects the physical essence of the monsoon, so is a suitable parameter to determine the mean monsoon onset and retreat. Based on the significant positive correlation between synoptic P and W, the interannual variations of the monsoon onset and retreat can also be determined from W. With transitional periods between summer and winter monsoons considered, the constant threshold taken in the criterion of the GUMI is suitable to the typical monsoons.

D.2 Introduction

A globally unified monsoon index (GUMI) was proposed in our earlier work (Zeng and Lu 2004) by using a single parameter [i.e., precipitable water (W)] and an objective criterion. The principle is to use the annual cycle of W to represent the annual monsoon process including the summer and winter monsoons and the transitions between them, and regard the monsoon onset and retreat as phase-locked phenomena, with each corresponding to a relatively fixed stage of the annual cycle. The global monsoon onset and retreat dates calculated from the GUMI are in general very close to those obtained from the local indexes. The GUMI has generated interests in the monsoon community (e.g., Li and Chen 2005; Liu et al. 2005), however, to ensure its reliability in monsoon research, some issues need to be clarified.

First, the rationality of using W to determine the monsoon onset and retreat should be confirmed, although W has already been adopted for this purpose in both research and weather prediction. For example, Cadet (1986) used the W to study the Indian monsoon onset. The National Weather Service in Arizona previously used the W to determine the monsoon onset and retreat in the southwest U.S. Although now the surface dewpoint is used (Randel et al. 1996), it has a very high correlation with the W (e.g., Lowry and Glahn 1969; Tomasi 1977; Viswanadham 1981). Conventionally, however, the precipitation (P) is the parameter utilized to determine the monsoon onset and retreat (e.g., Das 1987; Tao and Chen 1987; Hendon and Liebmann 1990; Douglas et al. 1993; Murakami and Matsumoto 1994). As a fundamental climate quantity that can be

observed from the surface, the P can not only seriously affect the human life (e.g., the floods and droughts influencing the agriculture), but also reflect the physical essence of the monsoon (i.e., the P is a product of and has an interaction with the monsoon circulations). In this study, it will be demonstrated that the W can reflect both the means and the interannual variations of the monsoon onset and retreat obtained from the P. Second, it was initially hoped that the global monsoon regions could be obtained from W along with the monsoon onset and retreat dates, but finally we found that they could not, and the reasons should be analyzed. Third, the rationality of the threshold taken in the criterion of the GUMI needs to be presented.

D.3 Relation between P and W

The P (mm/day) and W (mm) are two observed hydrological quantities. In the atmospheric water balance equation, the P corresponds to the time change rate of W, not the W itself. The relation between these two quantities is of a great concern to the hydro-climate community, but has not been well investigated. The data used in this study are the ten-year (1988-97) daily analyses of W and P over the continental United States and Mexico (US-Mexico) at a 1°×1° resolution, which are obtained respectively from the NASA Water Vapor Project (Randel et al. 1996) and the Climate Prediction Center of NOAA (e.g., Higgins et al. 1999). Denote the original data of P, for example, at a grid point as $P(d, y)$, where y is the year changing from 1 to 10 and d is the day of the year from 1 to 365. The mean annual cycle $P(d)$, obtained by averaging the original time

series over y, primarily reflects the seasonal changes. The daily deviation $p(d, y)$, obtained by removing the mean annual cycle from the original time series, primarily reflects the day-to-day or synoptic variations.

D.3.1 Seasonal Relation

Figure D.1 presents the mean annual cycles of P and W at 123°W/46°N in the western coast of the U.S. (WC), 105°W/21°N in South Mexico (SM), and 90°W/33°N in the southeastern U.S. (SE), which are the centers of the maximal standard deviation of the ten-year mean daily P over the US-Mexico (Fig. 1 in Lu and Zeng 2005). The W at the three locations has the same seasonal pattern of having an increase from winter to summer. Lu et al. (2005) revealed analytically that, for the seasonal change over the land of mid-high latitudes (e.g., the US-Mexico), because of the large annual range of the surface and air temperature, the W always increases seasonally with the temperature, both increasing from winter to summer.

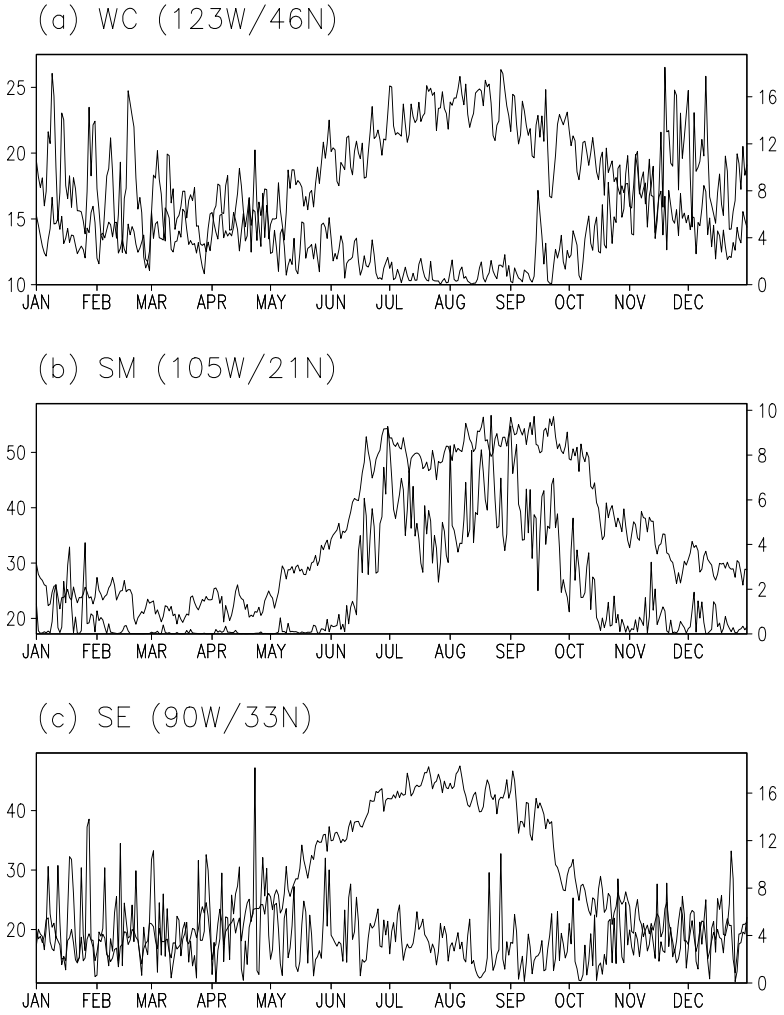

Figure D.1: Ten-year (1988-97) averaged daily analysis of precipitable water (thin, left axis, unit: mm) and precipitation (thick, right axis, unit: mm/day) at (a) WC, (b) SM, and (c) SE.

The different seasonal patterns of the P in Fig. D.1 represent the three major P seasonality regimes over the US-Mexico. Since the saturation of water vapor is a critical condition of P, the variation of P is found to be closely related to that of the relative humidity (denoted as $P \sim RH$; Lu and Zeng 2005). The relative humidity increases with vapor pressure (e) and decreases with temperature ($RH \sim e/T$), and hence $P \sim e/T$. To compare the relative significance of the seasonal changes of the two different variables (e and T) and their influences on the change of P, two dimensionless numbers, $C_{vap} \equiv e^{sum} / e^{win}$ and $C_{tem} \equiv e_s(T^{sum}) / e_s(T^{win})$, were defined to reflect the changes of water vapor and temperature from winter to summer. It is found that in WC, although the water vapor increases from winter to summer, the increase in temperature is much greater. So, the change of the P from winter to summer is mainly conversely affected by the change of temperature ($P \sim 1/T$). Since the W increases with temperature ($W \sim T$), the seasonal P and W have an out-of-phase relation ($P \sim 1/W$) as shown in Fig. D.1a. In SM, a monsoon area, the change of water vapor is much greater than the change of temperature. So, the seasonal change of P mainly depends on the change of water vapor ($P \sim e$). Note that the seasonal change of e in a level can largely represent the change of W ($e \sim W$), so the seasonal P and W have an in-phase relation ($P \sim W$) as shown in Fig. D.1b. In SE, the changes of water vapor and temperature are roughly equivalent ($e \sim T$), so the P does not change much from winter to summer ($P \sim const$), and thus has no significant relation with W (Fig. D.1c).

Figure D.2a is the distribution of the correlation between $P(d)$ and $W(d)$, representing the seasonal P and W. The correlation coefficient at a 95% confidence level by a simple Student's t-test is 0.10. The out-of-phase relation between the seasonal P and W, with a decrease of P but an increase of W from winter to summer, exists in the northwestern U.S. The in-phase relation, with an increase for both P and W from winter to summer, extends from Mexico to the Great Plains and the northern tier of the U.S. A lower correlation, with W increasing from winter to summer but P changing little throughout the year, appears in the southeastern U.S. Figure D.2b is the ten-year averaged difference of the monthly mean P between August and February. It shows that the larger P increase from winter to summer is mainly over the North American monsoon region.

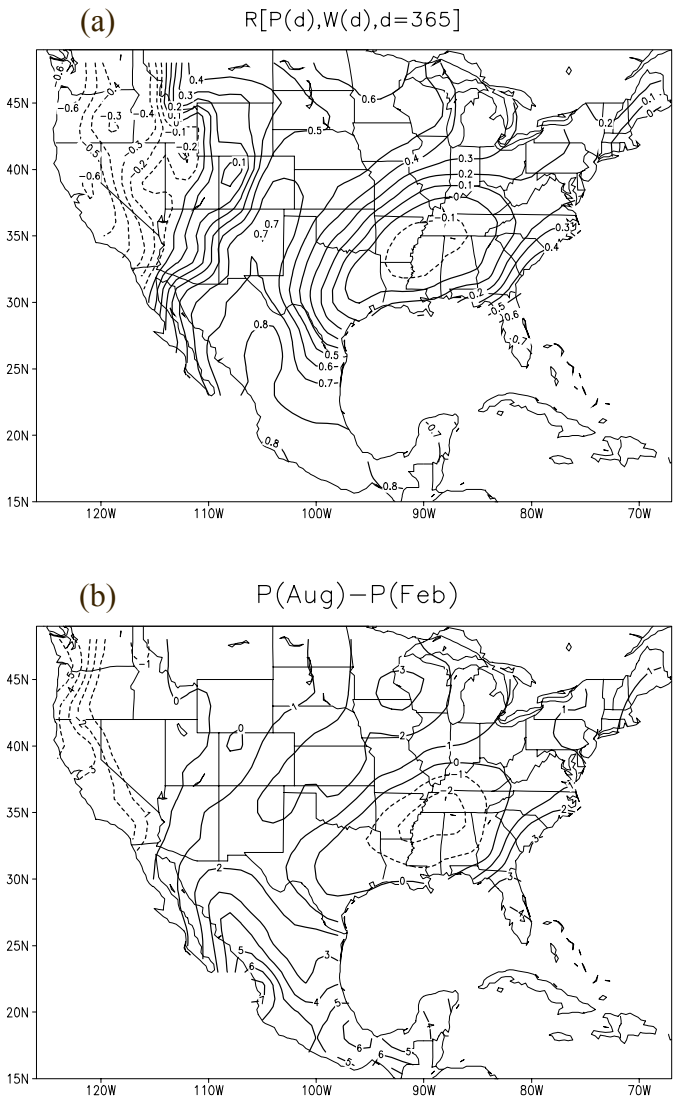

Figure D.2: (a) Distribution of the correlation between the ten-year (1988-97) averaged time series of daily P and W. (b) Difference of the ten-year averaged monthly mean P between August and February (unit: mm/day).

D.3.2 Synoptic Relation

Figure D.3a is the distribution of the correlation between the time series of $p(d, y)$ and $w(d, y)$, roughly representing the synoptic variations of P and W. The correlations in all the grid cells of the US-Mexico are positive, and the maximal correlation occurs in part of the monsoon region (the southwestern U.S. and northern Mexico). Actually, the synoptic P and W are positively correlated in any season. Figure D.3b is the correlation during the summer monsoon onset season (May 1 – July 31), and the coefficients are much greater than 0.20, the coefficient at the 95% confidence level.

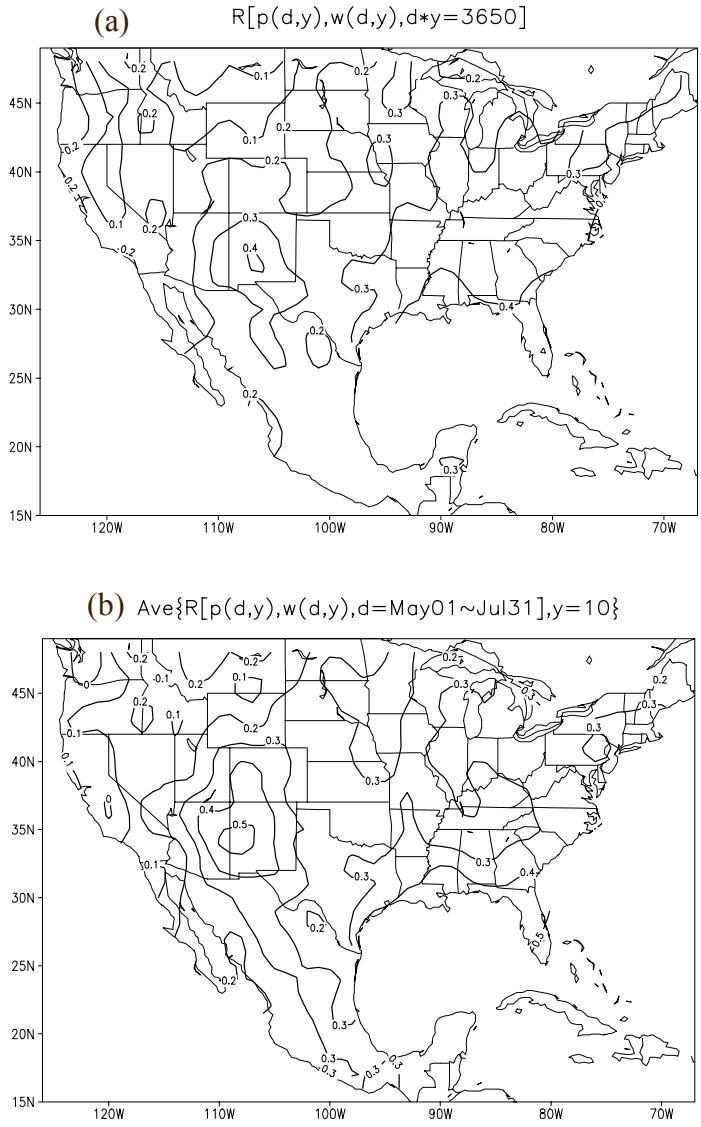

Figure D.3: Distribution of correlation coefficient between $p(d,y)$ and $w(d,y)$, the daily deviation of P and W. (a) Ten-year time series, and (b) Ten-year average for the monsoon onset season (May 1-July 31).

D.4 Clarification of the Issues

D.4.1 Rationality of Using W

The parameter conventionally used for determining the monsoon onset and retreat is the P, and the most important reason is that, as a product of the monsoon circulation, the P can reflect the physical essence of the monsoon. Generally, for any meteorological parameter, in order to become an effective indicator of monsoon onset and retreat, it should be able to determine both the means and the interannual variations of the onset and retreat dates as obtained from the P. The rationality of using the W for the determination of the monsoon onset and retreat can be confirmed from the seasonal and synoptic relations between P and W as revealed in section D.3.

In monsoon regions, P and W both increase from winter to summer. Moreover, the increases of the P and W during the transitional period from spring to summer both have positive responses to the increase of the land surface temperature, thus the land-ocean thermal contrast (since ocean surface temperature increases slowly). So, the W can also reflect the physical essence of the monsoon, and is suitable to be used to indicate the climatic monsoon onset and retreat.

The significant positive correlation between the synoptic P and W during the monsoon onset season (Fig. D.3b) implies that a larger (smaller) daily W statistically corresponds to a larger (smaller) daily P. So, an earlier (later) onset and retreat

determined from P can also be determined from W. Therefore, the interannual variation of the monsoon onset and retreat can be indicated by using the W.

D.4.2 Global Monsoon Regions

It was also attempted in Zeng and Lu (2004) to determine the global monsoon regions by using the single parameter W, with the hope to first decide if a grid point is located in a monsoon region, and, if it is, then determine its onset and retreat dates. When all the global monsoon regions were included by choosing a suitable critical value for the increase of W from winter to summer, some non-monsoon areas (the gray-shaded areas in Figs. 2 and 3 in Zeng and Lu 2004) were also included, which was removed subjectively.

From the analysis in section D.3, W always increases from winter to summer in mid-high latitudes where the surface temperature has a large annual range. The large increase of W from winter to summer can appear in both the monsoon and the nonmonsoon regions. Therefore, when the increase of W from winter to summer is used as the only criterion to determine the global monsoon regions, these nonmonsoon regions will also be included. Instead, the large increase of P from winter to summer occurs only in monsoon regions (Fig. D.2b), but it is also difficult to determine the monsoon regions from P alone.

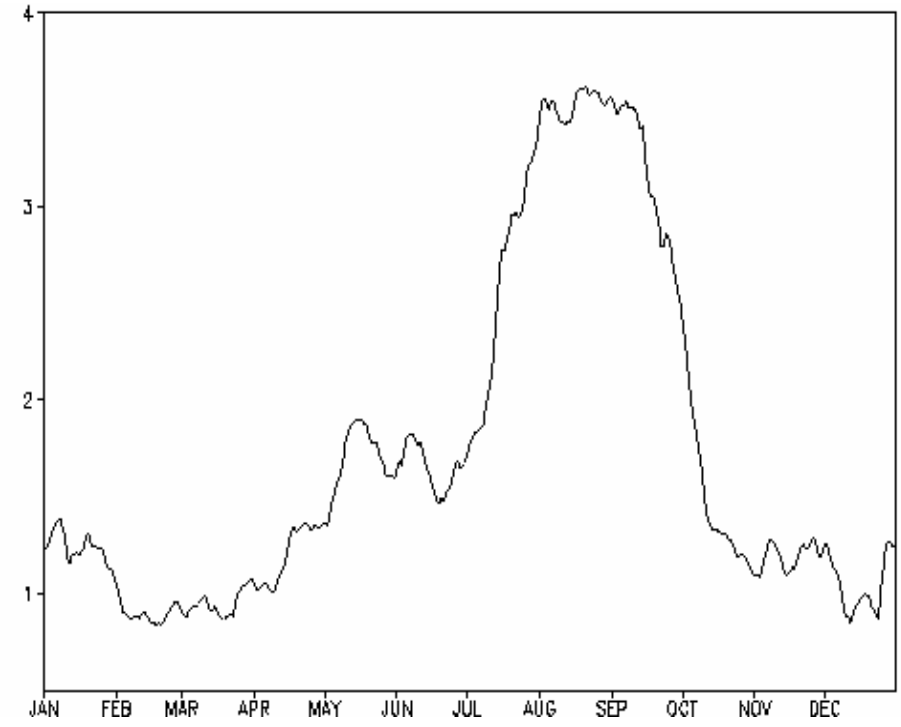

Figure D.4: Ten-year (1988-97) averaged daily W (unit: cm) in southern Arizona (111°W, 32°N) smoothed with a 9-day running mean.

D.4.3 Rationality of the Threshold

The index in the GUMI is defined as the daily W of a grid point normalized in a year so that it varies between 0 and 1. The onset (retreat) date for all the global monsoons is defined as the time when the unified monsoon index reaches (decreases to) a threshold of the golden number (0.618), to which some notes have already been given in Zeng and Lu (2004). This semi-empirical threshold is more reasonable than those using a critical value of 0.5, which lacks the transitions between the summer and winter monsoons, e.g., Fasullo and Webster (2003) although they were aware of the issue. As an estimate, a monsoon year can be symmetrically divided into a summer monsoon with the index greater than 0.618, a winter monsoon with index less than 0.382, and two transitional periods corresponding to the index between 0.382 and 0.618. If a sine wave is assumed to represent the annual cycle of the index, the summer and winter monsoons each lasts 3.5 months, and the transitional period is 2.5 months. Moreover, for most typical monsoons, e.g., the monsoon in southern Arizona (Fig. D.4), the onset or retreat is a rapid process occurring within just a few days, and the index increases from lower values to higher values promptly. So, the determination of the onset and retreat dates is not sensitive to the choice of the threshold. For the non-typical monsoons (e.g., near the edge of monsoon regions), the onset or retreat is a longer process during which the index increases or decreases slowly and with perturbations, so the onset and retreat dates are sensitive to the threshold.

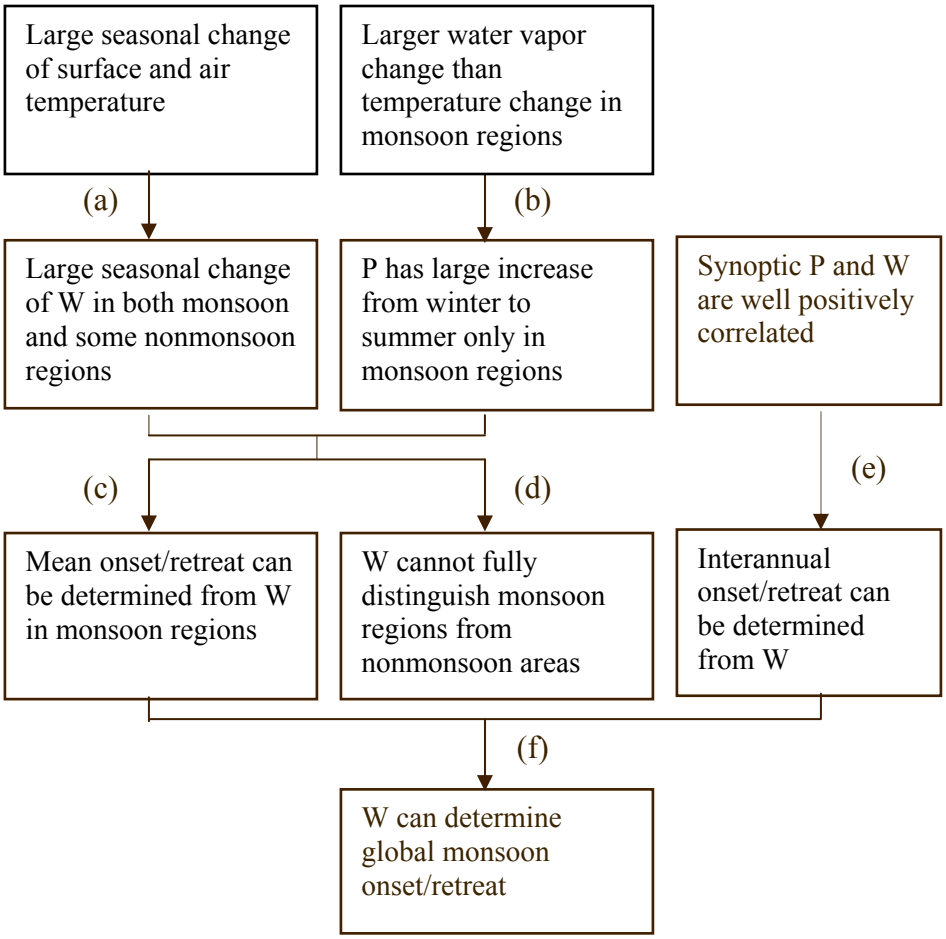

Figure D.5: A schematic illustrating the clarification of the issues in the GUMI.

D.5 Summary

To ensure the reliability of the GUMI constructed with W, three issues are clarified in this study. The relation between P and W, though is only for the US-Mexico, is helpful to the explanations of the rationality of using W to determine the monsoon onset and retreat and the reason why the global monsoon regions cannot be exactly identified from W. The main results can be summarized schematically as in Fig. D.5.

When the annual range of surface and air temperature is large, e.g., in mid-high latitudes, especially over land, the water vapor (W and e) always increases from winter to summer (Fig. D.5a). The different P seasonality regimes are determined by the comparative significance of the seasonal changes of water vapor and temperature. For instance, in the North American monsoon region, the change of water vapor is much greater than the change of temperature (Fig. D.5b). In monsoon regions, P and W have an in-phase relation, and both increase from winter to summer. During the monsoon onset season, they both respond positively to the increase of the surface temperature, so can reflect the physical essence of the monsoon. Therefore, the W is suitable to indicate the climatic monsoon onset and retreat (Fig. D.5c). In nonmonsoon regions, P and W no longer have the in-phase relation (maybe out-of-phase or not significantly correlated). Although P does not increase from winter to summer, W still does. Therefore, it is impossible to distinguish the global monsoon regions from the nonmonsoon regions from the seasonal change of W (Fig. D.5d). The synoptic P and W are always well and positively correlated. In monsoon regions, the earlier or later monsoon onset and retreat

determined by P in a specific year can also be determined from W. So, in addition to the mean, the interannual variation of the monsoon onset and retreat can also be determined from W (Fig. D.5e), which confirms the rationality of using the W to indicate the monsoon onset and retreat (Fig. D.5f). The rationality of the threshold taken in the criterion of the GUMI is that it makes the year contains both the summer and winter monsoons and the two transitions.

D.6 Acknowledgments

This work was supported by NOAA under grants NA06GP0569 and NA16GP1619 and NASA under the EOS/IDS program (429-81-22). The precipitable water and precipitation analysis data are distributed by the NASA/DAAC and NCEP/CPC, respectively.

D.7 References

Cadet, D. L., 1986: Fluctuations of precipitable water over the Indian Ocean during the 1979 summer monsoon. *Tellus.,* 38A, 170–177.

Das, P. K., 1987: Short- and long-range monsoon prediction in India. *Monsoons,* J. S. Fein and P. L. Stephens, Eds., John Wiley & Sons, 549–778.

Douglas, M., Maddox R. A., Howard K., and Reyes S., 1993: The Mexican monsoon. *J. Climate.,* 6, 1665–1677.

Fasullo, J. and P. J. Webster, 2003: A hydrological definition of Indian monsoon onset and withdrawal. *J. Climate*, 16, 3200–3211.

Hendon, H. H., and Liebmann B., 1990: A composite study of onset of the Australian summer monsoon. *J. Atmos. Sci.,* 47, 2227–2240.

Higgins, R. W., Y. Chen, and A. V. Douglas, 1999: Interannual variability of the North American warm season precipitation regime. *J. Climate*, 12, 653–680.

Li, H., and B. Chen, 2005: The evolution of precipitable water associated with the Asian and Australian monsoons as revealed from MODIS/SSMI, ECMWF and NCEP reanalysis data sets. *Geophys. Res. Lett.*, 32, L10811, doi:10.1029/2005GL022570.

Liu, B., M. Xu, M. Henderson, and Y. Qi, 2005: Observed trends of precipitation amount, frequency, and intensity in China, 1960–2000. *J. Geophys. Res.*, 110, D08103, doi:10.1029/2004JD004864.

Lowry, D. A., and H. R. Glahn, 1969: Relationships between integrated atmospheric moisture and surface weather. *J. Appl. Meteor.,* 8, 762–768.

Lu, E., and X. Zeng, 2005: Understanding different precipitation seasonality regimes from water vapor and temperature fields: Case studies. *Geophys. Res. Lett.*, in press.

Lu, E., X. Zeng, and M. Barlage, 2005: Change of precipitable water corresponding to surface temperature increase of varying scale: Theoretical analyses. *Geophys. Res. Lett.*, submitted.

Murakami, T., and Matsumoto J., 1994: Summer monsoon over the Asian continent and western North Pacific. *J. Meteor. Soc. Japan.,* 72, 719–745.

Randel, D. L., Vonder Haar T. H., Ringerud M. A., Stephens G. L., Greenwald T. J., and Combs C. L., 1996: A new global water vapor dataset. *Bull. Amer. Meteor. Soc.,* 77, 1233–1246.

Tao, S., and Chen L., 1987: A review of recent research on the East Asian summer monsoon in China. *Monsoon Meteorology,* C.-P. Chang and T. N. Krishnamurti, Eds., Oxford University Press, 60–92.

Tomasi, C., 1977: Precipitable water vapor in atmospheres characterized by temperature inversions. *J. Appl. Meteor.,* 16, 237–243.

Viswanadham, Y., 1981: The relationship between total precipitable water and surface dew point. *J. Appl. Meteor.,* 20, 3–8.

Zeng, X., and E. Lu, 2004: Globally unified monsoon onset and retreat indexes. *J. Climate*, 17, 2241-2248.

APPENDIX E

RECENT PUBLICATIONS

(since 1999)

Lu, E. and J. C. L. Chan, 1999: A unified monsoon index for South China. *J. Climate*, 12, 2375-2385.

Li, T., Y. Zhang, **E. Lu**, and D. Wang, 2002: Relative role of dynamic and thermodynamic processes in the development of the Indian Ocean dipole: An OGCM diagnosis. *Geophys. Res. Letts.*, 29(23), 2110, doi:10.1029/2002GL015789.

Zeng, X. and **E. Lu**, 2004: Globally unified monsoon onset and retreat indexes. *J. Climate*, 17, 2241-2248.

Lu, E. and X. Zeng, 2005: Understanding different precipitation seasonality regimes from water vapor and temperature fields: Case studies. *Geophys. Res. Letts.,* 32, doi:10.1029/2005GL024333.

Pielke Sr., R.A., T. Matsui, G. Leoncini, T. Nobis, U. Nair, **E. Lu**, J. Eastman, S. Kumar, C. Peters-Lidard, Y. Tian, and R. Walko, 2005: A new paradigm for parameterizations in numerical weather prediction and other atmospheric models. *National Wea. Digest*, in press.

Lu, E. and X. Zeng, 2005: Change of precipitable water corresponding to surface temperature increase of varying scale: Theoretical analyses. *Geophys. Res. Letts.*, submitted.

Lu, E. and X. Zeng, 2005: A clarification of the issues in the globally unified monsoon index. *J. Climate*, submitted.